

Chemistry of C-Trimethylsilyl-Substituted Heterocarboranes. 17. Syntheses, Structures, and Reactivities of Bent-Sandwich, d⁰ Zirconacarboranes of the “Carbons Adjacent” C₂B₄ Carborane Systems

Colacot J. Thomas, Lei Jia, Hongming Zhang, Upali Siriwardane,[†]
John A. Maguire, Ying Wang, Karen A. Brooks, Vikram P. Weiss, and
Narayan S. Hosmane*

Department of Chemistry, Southern Methodist University, Dallas, Texas 75275

Received October 7, 1994[®]

The reaction of ZrCl₄ with *closو-exo*-Li(THF)-1-Na(THF)-2-(SiMe₃)-3-(R)-2,3-C₂B₄H₄ (R = SiMe₃, Me, H) in a benzene/THF solvent mixture produced 1-Cl-1-(THF)-2,2'-(SiMe₃)₂-3,3'-(R)₂-4,4',5,5'-Li(THF)-1,1'-*commo*-Zr(2,3-C₂B₄H₄)₂ (R = SiMe₃ (**I**), Me (**II**), H (**III**)), in 68%, 61%, and 59% yields, respectively. Compound **I** was found to be resistant to chloride substitution with common alkylating agents. Instead, the reaction of **I** with Me₃SiCH₂-MgCl in a 1:1 molar ratio in a THF/Et₂O solvent mixture produced, in 40% yield, the salt [Mg(THF)₆][1-Cl-1-(THF)-2,2',3,3'-(SiMe₃)₄-1,1'-*commo*-Zr(2,3-C₂B₄H₄)₂]·4THF (**IV**), while a 1:2 molar reaction gave 1-Cl-1-(CH₂SiMe₃)-2,2',3,3'-(SiMe₃)₄-4,4',5,5'-[(μ-H)₄Li](μ₃-Cl)[Mg-(μ₂-Cl)(THF)₃]₂-1,1'-*commo*-Zr(2,3-C₂B₄H₄)₂ (**V**), in 65% yield. All compounds were characterized by chemical analyses, infrared spectroscopy, and ¹H, ¹¹B, and ¹³C NMR spectroscopy. Compounds **I**, **II**, and **V** were further characterized by ⁷Li NMR spectroscopy and **I**, **II**, **IV**, and **V** by single crystal X-ray diffraction. Compound **I** crystallizes as **I**-THF, in the triclinic space group *P*1, while **II**, **IV**, and **V** crystallized in the monoclinic space groups *P*2₁/c, *P*2₁/c, and *C*2/c, respectively. The unit cell parameters of **I**-THF are *a* = 11.428(3) Å, *b* = 12.140(3) Å, *c* = 17.685(4) Å, α = 93.27(2)°, β = 90.35(2)°, γ = 114.91(2)°, *V* = 2220.4(8) Å³, and *Z* = 2, while those of **II**, **IV**, and **V** are *a* = 16.928(8), 13.129(2), and 25.602 Å, *b* = 16.373(6), 22.429(5), and 22.541(4) Å, *c* = 12.048(5), 19.217(3), and 24.740(5) Å, β = 90.37(3), 90.16(2), and 90.17(2)°, *V* = 3339(2), 5660(2), and 14277(5) Å³, and *Z* = 4, 2, and 8, respectively. Full-matrix least-squares refinements of **I**-THF, **II**, **IV**, and **V** converged at *R* = 0.044, 0.059, 0.051, and 0.078 and *R*_w = 0.057, 0.073, 0.065, and 0.086, respectively.

Introduction

Because of their role in olefin polymerization systems, the d⁰ complexes of the type $[(\eta^5\text{-C}_5\text{R}_5)_2\text{M}(\text{L})]^+$ have received a great deal of attention.¹ Much of the research involved studies of the structural and electronic changes induced by different substituents on the cyclopentadienide ligands and the effect of those changes on the catalytic efficacy of the complex.² Another way to introduce structural and electronic changes is to replace the cyclopentadienide ligands with other cyclic six-electron π-donors. The carborane dianions of the type *nido*-[7,8-R₂C₂B₉H₉]²⁻ and *nido*-[2,3-R₂C₂B₄H₄]²⁻ (R = H or a cage carbon substituent) are formal six-electron donors and have ligating properties that are quite similar to those of the cyclopentadienides. Their simi-

larities to the Cp system have been demonstrated through the syntheses and structural characterizations of a number of sandwich and half-sandwich metalla-carborane complexes.³ However, within this group, examples of d⁰ transition-metal complexes are under-represented. Jordan and co-workers⁴ have reported the syntheses of several mixed-ligand complexes of the form Cp*(C₂B₉H₁₁)M(R) (M = Zr, Hf; R = anionic hydrocarbon unit; Cp* = C₅Me₅), with structures being reported for the complex where M = Zr and R = C(Me)=C(Me)₂ as well as for the dimer [Cp*(C₂B₉H₁₁)Zr]₂(μ-CH₂). The complexes were found to be similar to the parent zirconocenes in that they were bent-sandwich complexes in which both the Cp* and the carborane ligands were η⁵-bonded to the metal. More recently, Bercaw has reported the structures of two dimeric scandium complexes, {[Cp*(C₂B₉H₁₁)ScCH(SiMe₃)₂]₂Li}(THF)₃ and [Cp*(C₂B₉H₁₁)ScH]₂[Li(THF)₂]₂, which also showed bent-sandwich geometries.⁵ The scandium hydride complex was found to be surprisingly unreactive, presumably

* To whom correspondence should be addressed.

† Present address: Department of Chemistry, Louisiana Tech University, Ruston, LA 71272.

[®] Abstract published in *Advance ACS Abstracts*, February 1, 1995.

(1) (a) Jordan, R. F. *Adv. Organomet. Chem.* **1991**, 32, 325 and references therein. (b) Cardin, D. J.; Lappert, M. F.; Raston, C. L. *Chemistry of Organo-Zirconium and -Hafnium Compounds*; Ellis Horwood: West Sussex, England, 1986. (c) Kaminsky, W.; Sinn, H. *Transition Metals and Organometallics as Catalysts for Olefin Polymerization*; Springer-Verlag: Berlin, 1987 (see references therein).

(2) (a) Spaleck, W. A.; Antberg, M.; Rohrmann, J.; Winter, A.; Bachmann, B.; Kiprof, P.; Behm, J.; Herrmann, W. *Angew. Chem., Int. Ed. Engl.* **1992**, 31, 1347. (b) Kaminsky, W.; Kulper, K.; Bräntzinger, H. H.; Wild, F. R. W. P. *Angew. Chem., Int. Ed. Engl.* **1985**, 24, 507. (c) Woo, T. K.; Fan, L.; Ziegler, T. *Organometallics* **1994**, 13, 2252.

(3) (a) Hawthorne, M. F.; Young, D. C.; Wegner, P. A. *J. Am. Chem. Soc.* **1965**, 87, 1818. (b) Hanusa, T. P. *Polyhedron* **1982**, 1, 663. (c) Grimes, R. N. In *Comprehensive Organometallic Chemistry*; Wilkinson, G., Stone, F. G. A., Abel, E. W., Eds.; Pergamon: Oxford, U.K., 1982; Vol. 1, Chapter 5.5, p 459. (d) Hosmane, N. S.; Maguire, J. A. *Adv. Organomet. Chem.* **1990**, 30, 99.

(4) Crowther, D. J.; Baenziger, N. C.; Jordan, R. F. *J. Am. Chem. Soc.* **1991**, 113, 1455.

(5) Bazan, G. C.; Schaefer, W. P.; Bercaw, J. E. *Organometallics* **1993**, 12, 2126.

due to strong B–H–Sc bridges present in the dimer. There is even less information available on the smaller, C₂B₄-cage complexes. Grimes reported the structure of the air-stable complex (η^8 -C₈H₈)Ti[(C₂H₅)₂C₂B₄H₄] in which a titanium, in a formal +4 state, was sandwiched between the planar 10-electron donor, [C₈H₈]²⁻ and a *nido*-[(C₂H₅)₂C₂B₄H₄]²⁻ unit, with the cyclooctatetraenyl and the C₂B₃ bonding faces being essentially parallel to one another.⁶ This is in contrast to the structure of the mixed-ligand Ti(IV) sandwich 1-(η^5 -C₅H₅)-1-Cl-1-(THF)-2,3-(SiMe₃)₂-1,2,3-TiC₂B₄H₄, which has a bent-sandwich structure typical of the titanocenes.⁷ There have also been some very recent preliminary reports on several d⁰ mixed Cp-(R₂C₂B₄H₄) complexes of Nb and Ta, which show bent structures.⁸ To our knowledge, the only structural description of a full-sandwich, *commo*-metallacarborane of a d⁰ transition metal was that given in our preliminary report on the zirconacarborane 1-Cl-1-(THF)-2,2',3,3'-(SiMe₃)₄-4,5,5'-Li(THF)₂-1,1'-*commo*-Zr(2,3-C₂B₄H₄)₂.⁹ We report herein the details of the synthesis and structure of this compound as well as the C_{cage}-substituted derivatives along with the results of an investigation of their reaction chemistry, which turns out to be quite different from that of the mixed-ligand zirconium sandwich complexes or the zirconocenes.

Experimental Section

Materials. 2,3-Bis(trimethylsilyl)-2,3-dicarba-*nido*-hexaborane(8), 2-(trimethylsilyl)-3-methyl-2,3-dicarba-*nido*-hexaborane(8) and 2-(trimethylsilyl)-2,3-dicarba-*nido*-hexaborane (8), were prepared by the methods of Hosmane *et al.*¹⁰ ZrCl₄ (Aldrich Chemical Co.) was dried at 120 °C/10⁻⁴ mmHg for 12 h before use. Benzene, tetrahydrofuran (THF), diethyl ether (Et₂O), and n-hexane were dried over LiAlH₄ and doubly distilled before use. All other solvents were dried over 4–8 mesh molecular sieves (Aldrich) and either saturated with dry argon or degassed. Sodium hydride (NaH), *tert*-butyllithium (*t*-BuLi, 1.7 M solution in pentane), and Me₃SiCH₂MgCl (1 M solution in Et₂O) were obtained from Aldrich Chemical Co. and used as received. Solutions of the Na/Li complexes of the *nido*-carborane *clos*-*exo*-Li(THF)-1-Na(THF)-2-(SiMe₃)-3-(R)-2,3-C₂B₄H₄ (R = SiMe₃, Me, H) in THF/benzene mixture were prepared by the methods described elsewhere.¹¹

Spectroscopic and Analytical Procedures. Proton, lithium-7, boron-11, and carbon-13 pulse Fourier transform NMR spectra, at 200, 77.7, 64.2, and 50.3 MHz, respectively, were recorded on an IBM-WP200 SY multinuclear NMR spectrometer. Infrared spectra were obtained on a Perkin-Elmer Model 283 infrared spectrophotometer and a Nicolet Magna-550 FT-IR spectrophotometer. Elemental analyses were obtained from Oneida Research Services (ORS) Inc.,

(6) Swisher, R. G.; Sinn, E.; Grimes, R. N. *Organometallics* **1984**, 3, 599.

(7) Hosmane, N. S.; Wang, Y.; Zhang, H.; Maguire, J. A.; Waldhör, E.; Kaim, W.; Binder, H.; Kremer, R. K. *Organometallics* **1994**, 13, 4156.

(8) (a) Stockman, K. E.; Finn, M. G.; Sabat, M.; Grimes, R. N. Abstract No. 9, BUSA IV, Syracuse, NY, July 1994. (b) Houseknecht, K.; Finn, M. G.; Sabat, M.; Grimes, R. N. Abstract No. 68, BUSA IV, Syracuse, NY, July 1994.

(9) Siriwardane, U.; Zhang, H.; Hosmane, N. S. *J. Am. Chem. Soc.* **1990**, 112, 9637.

(10) (a) Hosmane, N. S.; Sirmokadam, N. N.; Mollenhauer, M. N. *J. Organomet. Chem.* **1985**, 279, 359. (b) Hosmane, N. S.; Mollenhauer, M. N.; Cowley, A. H.; Norman, N. C. *Organometallics* **1985**, 4, 1194. (c) Hosmane, N. S.; Maldar, N. N.; Potts, S. B.; Rankin, D. W. H.; Robertson, H. E. *Inorg. Chem.* **1986**, 25, 1561. (d) Hosmane, N. S.; Islam, M. S.; Burns, E. G. *Inorg. Chem.* **1987**, 26, 3236.

(11) (a) Hosmane, N. S.; Saxena, A. K.; Barreto, R. D.; Maguire, J. A.; Jia, L.; Wang, Y.; Oki, A. R.; Grover, K. V.; Whitten, S. J.; Dawson, K.; Tolle, M. A.; Siriwardane, U.; Demissie, T.; Fagner, J. S. *Organometallics* **1993**, 12, 3001. (b) Barreto, R. D.; Hosmane, N. S. *Inorg. Synth.* **1992**, 29, 89.

Whitesboro, NY, and E&R Microanalytical Laboratory, Inc., Corona, NY.

Synthetic Procedures. All experiments were carried out in Pyrex glass round-bottom flasks of 250 mL capacity, containing magnetic stirring bars and fitted with high-vacuum Teflon valves. Nonvolatile substances were manipulated in either a Vacuum Atmospheres drybox or evacuable glovebags under an atmosphere of dry nitrogen. All known compounds among the products were identified by comparing their mp/bp and IR and NMR spectra with those of the authentic samples.

Synthesis of 1-Cl-1-(C₄H₈O)-2,2'-(SiMe₃)₂-3,3'-(R)₂-4,4',5,5'-Li(C₄H₈O)-1,1'-*commo*-Zr(2,3-C₂B₄H₄)₂ (R = SiMe₃ (I**), Me (**II**), H (**III**)).** A benzene/THF solution (20 mL/1 mL) of *clos*-*exo*-Li(C₄H₈O)-1-Na(C₄H₈O)-2-(SiMe₃)-3-(R)-2,3-C₂B₄H₄ (1.76 g, 4.5 mmol, R = SiMe₃; 1.13 g, 3.4 mmol, R = Me; 1.31 g, 4.13 mmol, R = H) was poured onto anhydrous ZrCl₄ (0.52 g, 2.25 mmol; 0.39 g, 1.70 mmol; 0.42 g, 2.06 mmol) *in vacuo* at -78 °C, and the resulting heterogeneous mixture was stirred for 12 h, during which time the solution turned yellow. The solvents were then removed, the residue was dissolved in diethyl ether, and the mixture was stirred further for 30 min to precipitate NaCl out of the reaction mixture as an off-white solid. This mixture was filtered through a frit *in vacuo* to collect an orange filtrate. The solvent was removed from the filtrate under reduced pressure to obtain an orange-yellow solid which was identified as 1-Cl-1-(C₄H₈O)-2,2'-(SiMe₃)₂-3,3'-(R)₂-4,4',5,5'-Li(C₄H₈O)-1,1'-*commo*-Zr(2,3-C₂B₄H₄)₂ (1.20 g, 1.53 mmol, 68% yield, **I**; 0.70 g, 1.04 mmol, 61% yield, **II**; 0.78 g, 1.21 mmol, 59% yield, **III**). Compounds **I**–**III** are soluble in polar solvents and have melting points of 160, 141, and 134 °C, respectively. Anal. Calcd for C₂₄H₆₀B₈O₂ClSi₂LiZr (**I**): C, 40.44; H, 8.43; B, 12.13. Found: C, 40.20; H, 8.24; B, 12.39. Calcd for C₂₀H₄₈B₈O₂ClSi₂LiZr (**II**): C, 40.27; H, 8.05; Li, 1.10; Si, 9.41. Found: C, 40.65; H, 8.33; Li, 0.96; Si, 9.49. Calcd for C₁₈H₄₄B₈O₂ClSi₂LiZr (**III**): C, 38.00; H, 7.80; Li, 1.20. Found: C, 37.27; H, 7.32; Li, 0.95. While compound **I** was recrystallized from dry THF to form a THF-solvated species, **I**-THF, **II** was recrystallized from anhydrous benzene solution and was subsequently used for X-ray analyses.

Reaction of **I with Me₃SiCH₂MgCl (in 1:1 Mole Ratio).** A THF (20 mL) solution of 1-Cl-1-(C₄H₈O)-2,2',3,3'-(SiMe₃)₄-4,4',5,5'-Li(C₄H₈O)-1,1'-*commo*-Zr(2,3-C₂B₄H₄)₂ (**I**; 3.30 g, 4.23 mmol) was added to an ether solution of Me₃SiCH₂MgCl (1 M, 4.23 mL) *in vacuo* at -78 °C, over a period of 30 min. The reaction mixture was slowly warmed to room temperature with constant stirring, which continued for another 48 h. The mixture was then filtered *in vacuo* to remove some insoluble white solid (uncharacterized). Removal of solvents from the filtrate resulted in the formation of a fine, yellow fluffy (crystallite) material. Upon addition of 20 mL of C₆H₆, the crystallite dissolved readily, with immediate formation of an almost colorless crystalline solid. When this product was recrystallized from THF, pale yellow crystals formed slowly. Subsequent analysis showed the final product to be the salt [Mg(THF)₆][1-Cl-1-(C₄H₈O)-2,2',3,3'-(SiMe₃)₄-1,1'-*commo*-Zr(2,3-C₂B₄H₄)₂]·2⁺THF (**IV**; 3.4 g, 1.69 mmol, 40% yield; mp 96 °C dec). Anal. Calcd for C₈₀H₁₈₄B₁₆O₁₂Cl₂Si₈MgZr₂ (**IV**): C, 47.73; H, 9.23; Mg, 1.21. Found: C, 47.50; H, 9.40; Mg, 1.23. The X-ray-quality crystals of **IV** were grown from THF solution.

Reaction of **I with Me₃SiCH₂MgCl (in 1:2 Mole Ratio).** An Et₂O/THF (25 mL/5 mL) solution of **I** (3.30 g, 4.23 mmol) was added over a period of 30 min, with constant stirring, to an Et₂O solution of Me₃SiCH₂MgCl (1 M, 8.5 mL) *in vacuo* at -78 °C. The reaction mixture was slowly warmed to room temperature and was stirred for about 3 days, during which time no observable color change occurred. After 3 days, the solvent was removed under reduced pressure to obtain a gray-white crystallite material, which was redissolved in a mixture of C₆D₆ and CDCl₃ (5 mL/5 mL). Removal of solvents from the solution produced a gelatinous solid, which on treatment

Table 1. Crystal Data^a for I-THF, II, IV and V

	I-THF	II	IV	V
formula	C ₂₈ H ₆₈ O ₃ B ₈ Si ₄ ClLiZr	C ₂₀ H ₄₈ O ₂ B ₈ Si ₂ CLiZr	[C ₂₀ H ₅₂ OB ₈ Si ₄ ClZr] ₂ - [MgC ₂₄ H ₄₈ O ₆] ₄ THF	[C ₄₄ H ₁₀₃ O ₆ B ₈ Si ₅ Cl ₄ - LiMg ₂ Zr] _{1/2} Et ₂ O
fw	785.3	596.9	2013.6	1280.8
cryst system	triclinic	monoclinic	monoclinic	monoclinic
space group	P̄1	P2 ₁ /c	P2 ₁ /c	C2/c
<i>a</i> , Å	11.428(3)	16.928(8)	13.129(2)	25.602(6)
<i>b</i> , Å	12.140(3)	16.373(6)	22.429(5)	22.541(4)
<i>c</i> , Å	17.685(4)	12.048(5)	19.217(3)	24.740(5)
β , deg ^d	90.35(2)	90.37(3)	90.16(2)	90.17(2)
<i>V</i> , Å ³	2220.4(8)	3339(2)	5660(2)	14277(5)
<i>Z</i>	2	4	2	8
<i>D</i> _{calcd} , Mg/m ³	1.174	1.187	1.182	1.191
abs coeff, mm ⁻¹	0.435	0.489	0.370	0.442
crystal dimens, mm	0.25 × 0.20 × 0.15	0.20 × 0.30 × 0.05	0.20 × 0.30 × 0.10	0.05 × 0.30 × 0.15
scan type	$\theta/2\theta$	$\theta/2\theta$	w/ θ	w/ θ
scan speed in ω : min, max	5.0, 25.0	6.0, 30.0	6.0, 30.0	6.0, 30.0
2 θ range, deg	3.0–46.0	3.0–40.0	3.5–42.0	3.5–38.0
T, K	298	230	230	230
decay, %	0	0	0	0
no. of data collected	6556	3509	6413	5947
obsd refns, $I > 3.0\sigma(I)$	4842	2363	3813	3195
no. of params refined	415	292	523	652
GOF	2.01	2.93	1.44	1.66
<i>g</i> ^e	0.0003	0.0003	0.001	0.001
$\Delta Q_{\text{max}, \text{min}}$, e/Å ³	+0.64, -0.70	+0.63, -0.41	+0.65, -0.53	+0.56, -0.41
<i>R</i> ^b	0.044	0.059	0.051	0.078
<i>R</i> _w	0.057	0.073	0.065	0.086

^a Graphite-monochromatized Mo K α radiation, $\lambda = 0.71073$ Å. ^b $R = \sum |F_o| - |F_c| / \sum |F_o|$; $wR = [\sum w(F_o - F_c)^2 / \sum w(F_o)^2]^{1/2}$. ^c $w = 1 / [a^2(F_o) + g(F_o)^2]$.

^d For I, $\alpha = 93.27(2)^\circ$ and $\gamma = 114.91(8)^\circ$.

with diethyl ether (50 mL) resulted in a clear solution and an off-white solid residue (300 mg); the mixture was then filtered *in vacuo* to collect a pale yellow filtrate. The solid residue, collected on the frit, failed to burn with a green flame during the flame test, indicating the absence of boron in the residue; therefore, it was discarded. The filtrate was concentrated and allowed to stand in a vacuum flask at room temperature. On standing for 2 days, pale yellow crystals slowly formed from the filtrate and were identified as 1-Cl-1-(CH₂SiMe₃)-2,2',3,3'-(SiMe₃)₄-4,4',5,5'-[(μ-H)₄Li](μ₃-Cl)[Mg(μ₃-Cl)(THF)₃]₂-1,1'-*commo*-Zr(2,3-C₂B₄H₄)₂ (V; 3.16 g, 2.54 mmol, 65% yield; mp 145 °C). Anal. Calcd for C₄₄H₁₀₃B₈O₆Cl₄Si₅LiMg₂Zr (V): C, 42.49; H, 8.34; B, 6.96. Found: C, 42.33; H, 8.24; B, 7.14. The X-ray-quality crystals of V were grown from Et₂O solution.

X-ray Analyses of 1-Cl-1-(C₄H₈O)-2,2',3,3'-(SiMe₃)₄-4,5,5'-Li(C₄H₈O)₂-1,1'-*commo*-Zr(2,3-C₂B₄H₄)₂ (I-THF), 1-Cl-1-(C₄H₈O)-2,2'- (SiMe₃)₂-3,3'-(Me)₂-4,4',5,5'-Li(C₄H₈O)-1,1'-*commo*-Zr(2,3-C₂B₄H₄)₂ (II), [Mg(THF)₆][1-Cl-1-(C₄H₈O)-2,2',3,3'-(SiMe₃)₄-1,1'-*commo*-Zr(2,3-C₂B₄H₄)₂]₂·4THF (IV), and 1-Cl-1-CH₂SiMe₃-2,2',3,3'-(SiMe₃)₄-4,4',5,5'-[(μ-H)₄Li](μ₃-Cl)[Mg(μ₂-Cl)(THF)₃]₂-1,1'-*commo*-Zr(2,3-C₂B₄H₄)₂ (V). The crystals were coated with epoxy resin and mounted sequentially on a Siemens R3m/V diffractometer under a low-temperature nitrogen stream. The pertinent crystallographic data and conditions for data collection are summarized in Table 1. Final unit cell parameters were obtained by a least-squares fit of the angles of 24 accurately centered reflections ($15^\circ < 2\theta < 29^\circ$ for I-THF, $18^\circ < 2\theta < 30^\circ$ for II, $19^\circ < 2\theta < 26^\circ$ for IV, $16^\circ < 2\theta < 26^\circ$ for V). Three standard reflections, monitored after every 150 reflections, did not show any significant change in intensity during the data collection. The data were corrected for Lorentz and polarization effects. Semi-empirical absorption studies (ψ scan) were also applied, with the minimum and maximum transmission factors of 0.840 and 0.980 for I-THF, 0.659 and 0.820 for II, 0.723 and 0.756 for IV, and 0.725 and 0.764 for V, respectively. All structures were solved by heavy-atom methods and subsequent difference Fourier syntheses using the SHELXTL-Plus package.¹² Scattering factors, as well as anomalous-dispersion corrections for Zr, Mg, Cl, and

Si atoms, were taken from literature values.¹³ Full-matrix least-squares refinement was performed for each structure. Compounds II, IV, and V all showed disordered THF molecules that limited the extent to which these structures could be refined, at least compared to I-THF. In II the disoriented THF was one attached to the Li (labeled O(26)–C(30) in Table 2); in IV one of the four THF's of crystallization was disordered, while in V all six of the magnesium-coordinating THF's plus the ethyl groups of the Et₂O of crystallization were disordered. All of the disordered segments were elastically constrained in the final cycles of refinements. All carborane cage H atoms were located in DF maps, while the methyl and methylene H atoms, except the disordered ones, were placed at calculated positions. The final refinements converged at $R = 0.044$ and $R_w = 0.057$ for structure I-THF, 0.059 and 0.073 for II, 0.051 and 0.065 for IV, and 0.078 and 0.086 for V, respectively. The final atomic coordinates are given in Table 2; selected bond distances and bond angles are listed in Table 3. Additional geometric information is given in the supplementary material.

Results and Discussion

Synthesis. The reaction of ZrCl₄ with 2 equiv of the sodium/lithium compounds *closo-exo*-Li(THF)-1-Na-(THF)-2-(SiMe₃)-3-(R)-2,3-C₂B₄H₄ (R = SiMe₃, Me, H) in C₆H₆/THF mixtures produced the *commo*-zirconacarboranes 1-Cl-1-(THF)-2,2'- (SiMe₃)₂-3,3'-(R)₂-4,4',5,5'-Li(THF)-1,1'-*commo*-Zr(2,3-C₂B₄H₄)₂ (R = SiMe₃ (I), Me (II), H (III)), in 60–70% yields (see Scheme 1). One of the characteristics of these compounds is their ability, and tendency, to incorporate varying numbers of THF molecules of solvation, depending on the complex and conditions. The crystal structure of I-THF shows three THF molecules, two solvating the lithium and one coordinated to the zirconium (see Figure 1). However, the powdery sample of I sent for analysis clearly shows the presence of only two THF molecules, presumably

(12) Sheldrick, G. M. *Structure Determination Software Programs*; Siemens X-Ray Analytical Instruments Inc.: Madison, WI, 1991.

(13) International Tables for X-ray Crystallography; Kynoch Press: Birmingham, U.K., 1974; Vol. IV.

Table 2. Atomic Coordinates ($\times 10^4$) and Equivalent Isotropic Displacement Coefficients ($\text{\AA}^2 \times 10^3$)

	<i>x</i>	<i>y</i>	<i>z</i>	<i>U</i> (eq)		<i>x</i>	<i>y</i>	<i>z</i>	<i>U</i> (eq)
Compound I-THF									
Zr	2208(1)	3249(1)	2759(1)	38(1)	C(25)	6070(6)	1773(6)	1966(4)	85(3)
Li	-840(8)	742(8)	1763(5)	61(4)	C(26)	6140(6)	4156(6)	1608(4)	90(3)
Cl	4229(1)	5050(1)	3099(1)	58(1)	C(27)	3713(6)	7633(5)	2196(4)	86(3)
Si(1)	3911(2)	1595(1)	4100(1)	64(1)	C(28)	2472(8)	6967(6)	3659(4)	110(4)
Si(2)	5706(1)	3046(1)	2348(1)	56(1)	C(29)	885(7)	7083(6)	2362(6)	131(5)
Si(3)	2177(2)	6624(1)	2624(1)	73(1)	C(30)	4287(5)	5705(5)	873(3)	79(3)
Si(4)	2501(1)	4940(1)	767(1)	59(1)	C(31)	2109(7)	3711(6)	3(3)	90(3)
C(2)	3191(4)	1814(4)	3197(3)	46(2)	C(32)	1868(7)	6015(6)	433(4)	91(3)
C(3)	3919(4)	2411(4)	2519(3)	41(2)	O(40)	1635(3)	3138(3)	4004(2)	58(1)
B(4)	3006(5)	2108(5)	1804(3)	47(2)	C(41)	408(6)	2249(5)	4267(3)	79(3)
B(5)	1548(5)	1166(5)	2079(3)	53(2)	C(42)	241(10)	2738(9)	4983(5)	191(7)
B(6)	1724(6)	1039(5)	2983(4)	55(2)	C(43)	1262(10)	3857(8)	5171(5)	156(6)
B(7)	2868(6)	894(5)	2370(3)	52(2)	C(44)	2129(7)	4171(6)	4566(3)	89(3)
C(12)	1570(4)	4939(4)	2384(3)	50(2)	O(45)	-1777(5)	176(4)	800(3)	109(2)
C(13)	1697(4)	4277(4)	1664(3)	47(2)	C(46)	-2976(9)	-625(10)	659(6)	165(7)
B(14)	691(5)	2903(5)	1623(3)	50(2)	C(47)	-3588(13)	-442(16)	79(7)	274(17)
B(15)	-142(5)	2738(5)	2399(3)	51(2)	C(48)	-2587(21)	587(10)	-246(8)	330(21)
B(16)	475(5)	4064(5)	2869(4)	56(3)	C(49)	-1549(14)	662(14)	148(7)	486(18)
B(17)	162(5)	4037(5)	1889(4)	59(3)	O(50)	-1803(4)	-629(3)	2336(2)	75(2)
C(21)	4676(7)	3029(5)	4707(3)	91(3)	C(51)	-2486(8)	-699(6)	3004(5)	111(4)
C(22)	2621(7)	473(6)	4651(4)	99(4)	C(52)	-2772(11)	-1862(8)	3298(5)	149(6)
C(23)	5055(6)	900(6)	3937(4)	90(4)	C(53)	-2271(11)	-2470(8)	2791(7)	171(8)
C(24)	6808(5)	3873(5)	3175(3)	77(3)	C(54)	-1637(9)	-1712(6)	2227(6)	131(5)
Compound II									
Zr	2225(1)	503(1)	1326(1)	67(1)	B(15)	2350(8)	1109(8)	3279(10)	104(6)
Li	3719(13)	1010(14)	3028(21)	144(10)	B(16)	2659(6)	121(7)	3293(9)	84(5)
Cl	1516(1)	-595(1)	362(2)	83(1)	B(17)	1758(8)	359(9)	3979(11)	118(6)
Si(1)	2682(2)	375(2)	-1960(3)	109(1)	C(17)	414(6)	-235(6)	2782(9)	110(5)
Si(2)	1966(2)	-1544(2)	3197(2)	92(1)	C(18)	2921(5)	-1909(6)	2616(9)	108(5)
C(2)	2986(5)	493(5)	-498(8)	77(4)	C(19)	1923(7)	-1768(7)	4695(8)	133(6)
C(3)	3377(5)	-82(6)	286(9)	89(4)	C(20)	1171(6)	-2138(6)	2487(8)	116(5)
B(4)	3730(7)	309(7)	1312(12)	99(6)	O(21)	1388(3)	1438(3)	644(5)	80(2)
B(5)	3523(7)	1293(7)	1146(12)	100(5)	C(22)	561(5)	1283(6)	385(8)	89(4)
B(6)	3059(6)	1380(6)	8(11)	87(5)	C(23)	250(6)	2093(7)	6(9)	115(5)
B(7)	3924(7)	781(7)	18(13)	103(6)	C(24)	731(6)	2686(6)	631(10)	105(5)
C(7)	3594(6)	-936(6)	-101(9)	110(5)	C(25)	1492(6)	2316(5)	730(10)	105(5)
C(8)	3430(9)	814(10)	-2834(11)	205(9)	O(26)	4574(5)	1312(5)	3946(8)	134(4)
C(9)	2500(9)	-669(7)	-2373(10)	175(8)	C(27)	5307(7)	1391(21)	3629(15)	343(21)
C(10)	1760(7)	916(8)	-2191(10)	156(7)	C(28)	5746(11)	1751(18)	4457(18)	308(17)
C(12)	1932(5)	-396(5)	2999(6)	74(3)	C(29)	5258(9)	1917(17)	5333(14)	248(14)
C(13)	1234(6)	141(6)	2826(8)	86(4)	C(30)	4547(9)	1801(17)	4803(17)	333(19)
B(14)	1415(8)	1079(9)	2936(10)	102(6)					
Compound IV									
Zr	4517(1)	1583(1)	7655(1)	32(1)	O(41)	4776(4)	2337(2)	8433(3)	46(2)
Mg	10000	0	10000	37(1)	C(42)	5249(8)	2898(4)	8281(5)	71(4)
Cl	4943(2)	2221(1)	6640(1)	47(1)	C(43)	5639(12)	3122(5)	8954(7)	140(8)
Si(1)	2125(2)	2785(1)	7671(1)	49(1)	C(44)	5408(12)	2727(6)	9477(7)	122(7)
Si(2)	2330(2)	1749(1)	6084(1)	53(1)	C(45)	4753(8)	2260(4)	9195(4)	62(4)
Si(3)	5932(2)	341(1)	6382(1)	55(1)	O(51)	9886(4)	156(2)	11079(3)	47(2)
Si(4)	7521(2)	1660(1)	7066(1)	49(1)	C(52)	8937(6)	109(5)	11469(4)	69(4)
C(2)	2688(5)	2017(3)	7630(4)	38(3)	C(53)	9144(9)	374(8)	12144(5)	143(8)
C(3)	2781(5)	1628(4)	7003(4)	41(3)	C(54)	10194(8)	391(6)	12254(5)	93(5)
B(4)	3033(7)	965(4)	7224(5)	45(4)	C(55)	10690(7)	313(4)	11556(4)	63(4)
B(5)	3045(7)	952(4)	8094(5)	45(4)	O(56)	9659(4)	917(2)	9832(3)	49(2)
B(6)	2849(7)	1656(4)	8327(5)	42(3)	C(57)	9602(9)	1211(4)	9159(5)	78(4)
B(7)	2042(8)	1357(4)	7671(5)	50(4)	C(58)	9468(14)	1821(5)	9278(7)	153(9)
C(12)	5725(6)	789(3)	7202(4)	40(3)	C(59)	9374(11)	1950(5)	9994(7)	105(6)
C(13)	6382(5)	1292(5)	7471(4)	36(3)	C(60)	9441(7)	1369(3)	10348(5)	59(4)
B(14)	6211(7)	1374(4)	8263(5)	45(4)	O(61)	11548(4)	218(2)	10076(3)	45(2)
B(15)	5361(8)	879(5)	8502(5)	49(4)	C(62)	12394(6)	-186(4)	10206(5)	52(3)
B(16)	5052(7)	513(4)	7796(5)	45(4)	C(63)	13332(7)	143(4)	10064(6)	82(5)
B(17)	6364(8)	647(4)	7961(5)	47(4)	C(64)	13052(6)	775(4)	10183(6)	72(4)
C(21)	2047(8)	3041(4)	8588(5)	80(4)	C(65)	11977(7)	818(4)	9972(5)	60(4)
C(22)	2875(7)	3366(4)	7214(5)	72(4)	O(71)	7148(4)	1199(3)	11124(3)	66(2)
C(23)	792(7)	2782(4)	7339(5)	78(4)	C(72)	6536(7)	1556(4)	10697(5)	64(4)
C(24)	975(7)	1531(5)	6009(5)	88(5)	C(73)	5482(7)	1330(4)	10748(5)	63(4)
C(25)	3038(8)	1267(5)	5479(5)	93(5)	C(74)	5455(7)	1044(5)	11440(6)	91(5)
C(26)	2451(8)	2513(5)	5725(5)	83(5)	C(75)	6518(7)	972(4)	11658(5)	69(4)
C(27)	5075(9)	-314(4)	6388(5)	97(5)	O(76)	8070(10)	4268(9)	8968(9)	381(12)
C(28)	5667(8)	751(4)	5563(4)	81(4)	C(77)	8715(13)	4496(6)	9444(8)	278(12)
C(29)	7273(8)	34(4)	6359(5)	81(4)	C(78)	9727(11)	4352(7)	9214(9)	236(10)
C(30)	8673(6)	1228(5)	7347(5)	71(4)	C(79)	9547(11)	3779(6)	8903(8)	204(8)
C(31)	7557(7)	1714(4)	6094(4)	66(4)	C(80)	8472(11)	3719(7)	9023(8)	259(11)
C(32)	7656(7)	2437(4)	7398(5)	77(4)					

Table 2. (Continued)

	<i>x</i>	<i>y</i>	<i>z</i>	<i>U</i> (eq)		<i>x</i>	<i>y</i>	<i>z</i>	<i>U</i> (eq)
Compound V									
Zr	2628(1)	4873(1)	973(1)	67(1)	C(29)	3041(9)	3070(9)	2070(8)	200(16)
Li	3427(14)	6063(16)	863(11)	110(16)	C(30)	2893(10)	4371(10)	2803(8)	243(20)
Mg(1)	3997(2)	7893(3)	1352(2)	78(2)	C(31)	4051(12)	4098(14)	2564(10)	358(30)
Mg(2)	4782(2)	7230(2)	548(2)	70(2)	C(32)	3704(11)	5360(11)	2662(8)	282(23)
Cl(1)	2120(2)	4302(2)	1643(2)	107(2)	O(51)	4095(6)	8752(6)	1627(6)	116(7)
Cl(2)	4295(2)	8167(2)	434(2)	96(2)	C(52)	4567(8)	8917(8)	1876(13)	264(23)
Cl(3)	4923(2)	7587(2)	1494(2)	88(2)	C(53)	4598(7)	9577(9)	1859(9)	178(17)
Cl(4)	3926(2)	6863(2)	932(2)	84(2)	C(54)	4228(11)	9750(7)	1421(9)	225(21)
Si(5)	2578(2)	4326(2)	-466(2)	77(2)	C(55)	3844(7)	9253(10)	1410(9)	163(15)
C(41)	2389(6)	4307(6)	254(5)	65(7)	O(56)	3216(4)	8048(5)	1172(5)	98(6)
C(42)	1995(7)	4386(8)	-912(6)	106(9)	C(57)	3034(6)	8056(13)	635(4)	221(19)
C(43)	2907(7)	3639(7)	-666(7)	116(10)	C(58)	2470(7)	7897(10)	646(8)	150(13)
C(44)	3024(6)	4946(7)	-658(6)	101(9)	C(59)	2306(4)	8070(13)	1201(10)	215(19)
C(2)	1768(6)	5450(7)	832(7)	63(7)	C(60)	2792(6)	8022(20)	1530(5)	342(31)
C(3)	2033(7)	5710(8)	1301(7)	90(9)	O(61)	3804(4)	7623(8)	2126(4)	111(7)
B(4)	2549(10)	5992(9)	1145(8)	87(11)	C(62)	3851(10)	7040(6)	2323(8)	179(16)
B(5)	2627(8)	5883(9)	509(7)	68(9)	C(63)	3673(13)	7045(10)	2896(7)	189(17)
B(6)	2107(8)	5521(9)	315(8)	71(9)	C(64)	3536(12)	7671(14)	3025(5)	222(21)
B(7)	2019(9)	6131(10)	728(9)	85(11)	C(65)	3731(10)	8021(7)	2556(8)	250(22)
C(12)	3337(7)	4141(9)	1289(9)	98(10)	O(66)	5487(4)	7588(5)	267(5)	94(6)
C(13)	3382(8)	4643(10)	1656(8)	102(10)	C(67)	5513(6)	8150(7)	22(8)	166(14)
B(14)	3535(10)	5202(11)	1361(9)	96(11)	C(68)	6076(8)	8296(7)	-50(8)	150(13)
B(15)	3604(7)	5019(10)	724(8)	70(9)	C(69)	6338(5)	7936(9)	377(10)	167(15)
B(16)	3451(8)	4344(10)	676(8)	74(10)	C(70)	5979(7)	7427(9)	470(12)	238(20)
B(17)	3884(10)	4563(12)	1201(11)	112(13)	O(71)	5125(4)	6406(4)	708(6)	99(6)
Si(1)	1068(2)	5240(3)	758(3)	108(3)	C(72)	5414(7)	6056(9)	346(6)	225(19)
Si(2)	1766(4)	5936(3)	1978(3)	162(4)	C(73)	5379(10)	5431(7)	536(10)	196(18)
Si(3)	3308(3)	3318(3)	1407(3)	134(4)	C(74)	5253(10)	5488(8)	1121(10)	160(15)
Si(4)	3481(4)	4596(4)	2414(3)	201(6)	C(75)	5061(9)	6105(9)	1200(5)	153(14)
C(21)	913(6)	5114(8)	42(8)	133(12)	O(76)	4573(4)	6950(6)	-231(4)	92(6)
C(22)	907(6)	4548(7)	1096(8)	136(11)	C(77)	4245(8)	6455(8)	-296(7)	269(23)
C(23)	625(7)	5848(8)	964(9)	160(13)	C(78)	4174(9)	6360(9)	-888(9)	184(16)
C(24)	1509(10)	6727(9)	1933(10)	263(20)	C(79)	4306(15)	6945(12)	-1133(7)	258(22)
C(25)	1284(9)	5412(9)	2264(8)	217(16)	C(80)	4570(12)	7297(7)	-703(7)	213(18)
C(26)	2299(12)	5933(13)	2452(8)	313(28)	O(81)	5000	1645(17)	2500	346(20)
C(27)	2894(8)	2947(8)	909(8)	152(12)	C(82)	4745(14)	1940(9)	2082(12)	311(20)
C(28)	3976(9)	3026(10)	1346(10)	240(20)	C(83)	4510(12)	1485(15)	1729(12)	244(14)

^a Equivalent isotropic *U*, defined as one-third of the trace of the orthogonalized U_{ij} tensor.

one solvating a Li and the other bound to the Zr. The ¹³C NMR spectrum of the crystalline sample of **I** (**I**/THF) agrees more with the X-ray structure in that it shows two different sets of THF resonances, with 1:2 peak area ratios, one set at 76.43 and 33.24 ppm, due to the Zr-bound THF, and the other set, ascribed to the Li-bound molecules, having resonances at 68.63 and 25.49 ppm.⁹ On the other hand, the results found for **II**, in which a Me replaces a SiMe₃ on each of the carboranes, shows somewhat different results. Both the X-ray study and ¹³C and ¹H NMR spectra show two THF molecules, one each on the Li and Zr (see Figure 2 and Table 4). Although no X-ray data could be obtained for **III**, the analytical and NMR spectral data suggest that the structure of **III** is similar to that of **II** in that both have single THF molecules coordinating the Li and Zr atoms. The alterations in the appearances and characteristics of the solids found in the preparation and purification steps of **IV** and **V**, as described in the Experimental Section, are also what one would expect for species exhibiting variable solvation patterns.

The most surprising and, from a practical standpoint, disappointing results were the products obtained from the reactions of **I** with Me₃SiCH₂MgCl (see Scheme 1). A 1:1 molar ratio of **I** and the Grignard reagent resulted in the replacement of two Li⁺'s by a Mg²⁺, giving the ionic compound **IV** (Figures 3 and 4). The only major alteration is that a cation no longer occupies a bridging position on the zirconacarborane anions (see Figures 1

and 2). Reaction of **I** with excess Me₃SiCH₂MgCl resulted in the formation of a complex double salt, **V**, which is shown in Figure 5 and Scheme 1. The 65% yield of this compound indicates that **V** is the major solid product formed in this reaction. Compound **V** was also the only identified product of the reaction of the chlorozirconacarborane with the Grignard reagent, in that [Me₃SiCH₂]⁻ replaced the THF in the primary coordination sphere of the zirconium. The actual mass balances of the reactions of **I** with the Grignard reagent are not known. With the exception of the replacement of the one zirconium-bound THF by a Me₃SiCH₂ in **V**, the Grignard alkyl groups were not found among the products. Presumably, they react with some proton source in the reaction mixture and leave as Me₄Si. Also, the stoichiometry of compound **V** is such that it would require the reaction of 3 mol of Grignard reagent for every 1 mol of **V** formed, not the 2:1 molar ratio of the reaction; the 65% yield would allow for such a 3:1 stoichiometry. Compound **I** also failed to react with other standard alkylating agents such as AlMe₃, MeLi, *t*-BuLi, and Me₃SiCH₂Li. At this point it is not known whether compounds **IV** and **V** are the results of bonding preferences or solubility differences. Irrespective of the driving force, the results do demonstrate the inertness of the Cl that is coordinated to the zirconium; this is quite different from the behavior of corresponding chlorozirconocenes.¹

Table 3. Selected Bond Lengths (\AA) and Bond Angles (deg)^a

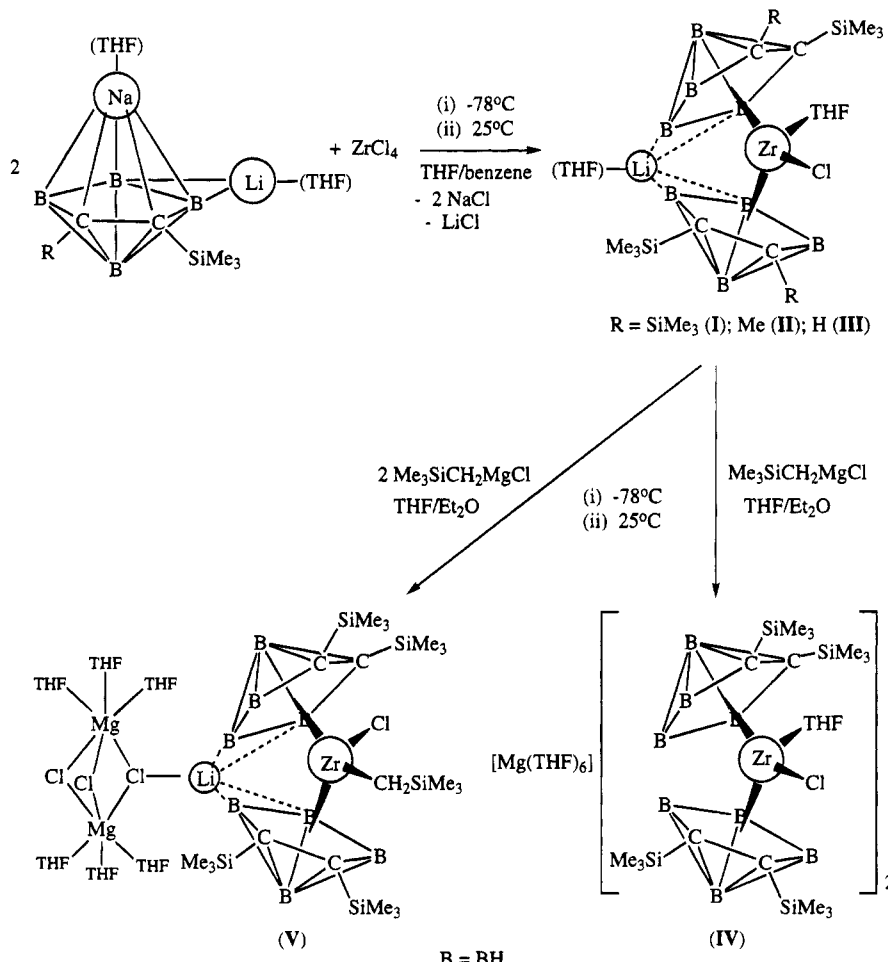
Bond Lengths						
Compound I-THF						
Zr-Cnt(1)	2.176	Zr-Cnt(2)	2.172	C(2)-B(6)	1.570(7)	C(2)-B(7)
Zr-Cl	2.461(1)	Zr-C(2)	2.587(6)	C(3)-B(4)	1.559(7)	C(3)-B(7)
Zr-C(3)	2.583(5)	Zr-B(4)	2.534(6)	B(4)-B(5)	1.670(7)	B(4)-B(7)
Zr-B(5)	2.538(6)	Zr-B(6)	2.557(6)	B(5)-B(6)	1.633(9)	B(5)-B(7)
Zr-C(12)	2.567(6)	Zr-C(13)	2.553(5)	B(6)-B(7)	1.762(9)	C(12)-C(13)
Zr-B(14)	2.542(6)	Zr-B(15)	2.556(6)	C(12)-B(16)	1.558(7)	C(12)-B(17)
Zr-B(16)	2.563(7)	Zr-O(40)	2.296(3)	C(13)-B(14)	1.574(6)	C(13)-B(17)
Li-B(5)	2.606(11)	Li-B(14)	2.494(6)	B(14)-B(15)	1.648(8)	B(14)-B(17)
Li-B(15)	2.413(10)	Li-O(45)	1.935(10)	B(15)-B(16)	1.632(8)	B(15)-B(17)
Li-O(50)	1.916(9)	C(2)-C(3)	1.502(6)	B(16)-B(17)	1.764(9)	
Compound II						
Zr-Cnt(3)	2.179	Zr-Cnt(4)	2.169	C(3)-B(4)	1.512(17)	C(3)-B(7)
Zr-Cl	2.450(2)	Zr-C(2)	2.554(9)	C(3)-C(7)	1.520(14)	B(4)-B(5)
Zr-C(3)	2.513(10)	Zr-B(4)	2.566(11)	B(4)-B(7)	1.773(20)	B(5)-B(6)
Zr-B(5)	2.559(11)	Zr-B(6)	2.570(11)	B(5)-B(7)	1.739(19)	B(6)-B(7)
Zr-C(12)	2.548(8)	Zr-C(13)	2.544(9)	C(12)-C(13)	1.485(13)	C(12)-B(16)
Zr-B(14)	2.563(12)	Zr-B(15)	2.561(12)	C(12)-B(17)	1.735(16)	C(13)-B(14)
Zr-B(16)	2.554(11)	Zr-O(21)	2.240(5)	C(13)-B(17)	1.682(16)	C(13)-C(17)
Li-B(4)	2.364(28)	Li-B(5)	2.335(28)	B(14)-B(15)	1.634(19)	B(14)-B(17)
Li-B(15)	2.344(26)	Li-B(16)	2.333(25)	B(15)-B(16)	1.700(18)	B(15)-B(17)
Li-O(26)	1.883(25)	C(2)-C(3)	1.487(13)	B(16)-B(17)	1.783(18)	
C(2)-B(6)	1.579(14)	C(2)-B(7)	1.766(14)			
Compound IV						
Zr-Cnt(5)	2.173	Zr-Cnt(6)	2.152	C(3)-B(4)	1.582(13)	C(3)-B(7)
Zr-Cl	2.485(2)	Zr-C(2)	2.592(7)	B(4)-B(5)	1.672(14)	B(4)-B(7)
Zr-C(3)	2.600(7)	Zr-B(4)	2.530(10)	B(5)-B(6)	1.660(14)	B(5)-B(7)
Zr-B(5)	2.541(10)	Zr-B(6)	2.551(9)	B(6)-B(7)	1.776(14)	C(12)-C(13)
Zr-C(12)	2.541(8)	Zr-C(13)	2.560(7)	C(12)-B(16)	1.573(12)	C(12)-B(17)
Zr-B(14)	2.552(9)	Zr-B(15)	2.523(10)	C(13)-B(14)	1.549(12)	C(13)-B(17)
Zr-B(16)	2.515(9)	Zr-O(41)	2.283(5)	B(14)-B(15)	1.642(14)	B(14)-B(17)
Mg-O(51)	2.109(5)	Mg-O(56)	2.129(5)	B(15)-B(16)	1.636(13)	B(15)-B(17)
Mg-O(61)	2.095(5)	C(2)-C(3)	1.493(11)	B(16)-B(17)	1.776(14)	
C(2)-B(6)	1.580(12)	C(2)-B(7)	1.709(13)			
Compound V						
Zr-Cnt(7)	2.196	Zr-Cnt(8)	2.222	Li-Cl(4)	2.216(36)	C(41)-Si(5)
Zr-Cl(1)	2.471(5)	Zr-C(41)	2.271(13)	C(42)-Si(5)	1.860(17)	C(43)-Si(5)
Zr-C(2)	2.580(15)	Zr-C(3)	2.558(18)	C(44)-Si(5)	1.867(17)	C(2)-C(3)
Zr-B(4)	2.567(20)	Zr-B(5)	2.551(19)	C(2)-B(6)	1.556(26)	C(2)-B(7)
Zr-B(6)	2.561(20)	Zr-C(12)	2.574(19)	C(3)-B(4)	1.518(30)	C(3)-B(7)
Zr-C(13)	2.614(20)	Zr-B(14)	2.617(24)	B(4)-B(5)	1.606(27)	B(4)-B(7)
Zr-B(15)	2.597(18)	Zr-B(16)	2.533(20)	B(5)-B(6)	1.633(28)	B(5)-B(7)
Mg(1)-Cl(2)	2.476(7)	Mg(1)-Cl(3)	2.492(7)	B(6)-B(7)	1.729(30)	C(12)-C(13)
Mg(1)-Cl(4)	2.547(7)	Mg(1)-O(51)	2.068(14)	C(12)-B(16)	1.612(30)	C(12)-B(17)
Mg(1)-O(56)	2.077(11)	Mg(1)-O(61)	2.070(12)	C(12)-Si(3)	1.878(22)	C(13)-B(14)
Mg(2)-Cl(2)	2.468(7)	Mg(2)-Cl(3)	2.499(7)	C(13)-B(17)	1.722(33)	C(13)-Si(4)
Mg(2)-Cl(4)	2.532(7)	Mg(2)-O(66)	2.096(12)	B(14)-B(15)	1.639(30)	B(14)-B(17)
Mg(2)-O(71)	2.092(11)	Mg(2)-O(76)	2.097(12)	B(15)-B(16)	1.576(31)	B(15)-B(17)
Li-B(4)	2.361(42)	Li-B(5)	2.263(39)	B(16)-B(17)	1.774(33)	
Li-B(14)	2.316(41)	Li-B(15)	2.421(41)			
Bond Angles						
Compound I-THF						
Cnt(1)-Zr-Cl	108.0	Cnt(2)-Zr-Cl	110.1	C(3)-B(7)-B(5)	95.3(4)	B(4)-B(7)-B(5)
Cnt(1)-Zr-O(40)	105.1	Cnt(2)-Zr-O(40)	104.9	C(2)-B(7)-B(6)	53.5(3)	C(3)-B(7)-B(6)
Cnt(1)-Zr-Cnt(2)	130.4	Cl-Zr-O(40)	90.5(1)	B(4)-B(7)-B(6)	95.9(5)	B(5)-B(7)-B(6)
B(5)-Li-B(14)	67.2(3)	B(5)-Li-B(15)	81.2(3)	C(13)-C(12)-B(16)	110.6(4)	C(13)-C(12)-B(17)
B(5)-Li-O(45)	128.0(5)	B(14)-Li-O(45)	105.7(4)	B(16)-C(12)-B(17)	65.0(3)	C(12)-C(13)-B(14)
B(15)-Li-O(45)	127.1(5)	B(5)-Li-O(50)	103.1(5)	C(12)-C(13)-B(17)	64.2(3)	B(14)-C(13)-B(17)
B(14)-Li-O(50)	153.8(5)	B(15)-Li-O(50)	117.3(5)	C(13)-B(14)-B(15)	105.7(4)	C(13)-B(14)-B(17)
O(45)-Li-O(50)	99.3(4)	C(3)-C(2)-B(6)	110.9(4)	B(15)-B(14)-B(17)	62.3(4)	B(14)-B(15)-B(16)
C(3)-C(2)-B(7)	64.2(3)	B(6)-C(2)-B(7)	64.4(3)	B(14)-B(15)-B(17)	62.1(4)	B(16)-B(15)-B(17)
C(2)-C(3)-B(4)	111.4(4)	C(2)-C(3)-B(7)	64.2(3)	C(12)-B(16)-B(15)	106.9(5)	C(12)-B(16)-B(17)
B(4)-C(3)-B(7)	65.4(3)	C(3)-B(4)-B(5)	105.6(4)	B(15)-B(16)-B(17)	62.6(4)	C(12)-B(17)-C(13)
C(3)-B(4)-B(7)	61.8(3)	B(5)-B(4)-B(7)	61.0(4)	C(12)-B(17)-B(14)	93.6(4)	C(13)-B(17)-B(14)
B(4)-B(5)-B(6)	105.6(4)	B(4)-B(5)-B(7)	62.6(4)	C(12)-B(17)-B(15)	94.8(4)	C(13)-B(17)-B(15)
B(6)-B(5)-B(7)	62.6(4)	C(2)-B(6)-B(5)	106.5(4)	B(14)-B(17)-B(15)	55.6(4)	C(12)-B(17)-B(16)
C(2)-B(6)-B(7)	62.1(3)	B(5)-B(6)-B(7)	62.1(4)	C(13)-B(17)-B(16)	93.1(4)	B(14)-B(17)-B(16)
C(2)-B(7)-C(3)	51.6(2)	C(2)-B(7)-B(4)	92.3(4)	B(15)-B(17)-B(16)	55.0(3)	Zr-O(40)-C(41)
C(3)-B(7)-B(4)	52.8(3)	C(2)-B(7)-B(5)	95.0(4)	Zr-O(40)-C(44)	124.0(3)	

Table 3 (Continued)

Bond Angles						
Compound II						
Cnt(1)–Zr–Cl	106.8	Cnt(2)–Zr–Cl	106.7	C(3)–B(7)–B(5)	92.1(8)	B(4)–B(7)–B(5)
Cnt(1)–Zr–O(21)	106.1	Cnt(2)–Zr–O(21)	104.3	C(2)–B(7)–B(6)	53.2(6)	C(3)–B(7)–B(6)
Cnt(1)–Zr–Cnt(2)	133.6	Cl–Zr–O(21)	91.2(2)	B(4)–B(7)–B(6)	95.2(8)	B(5)–B(7)–B(6)
B(4)–Li–B(15)	99.2(9)	B(5)–Li–B(15)	88.7(9)	C(13)–C(12)–B(16)	110.0(8)	C(13)–C(12)–B(17)
B(4)–Li–B(16)	80.0(8)	B(5)–Li–B(16)	98.8(9)	B(16)–C(12)–B(17)	65.8(7)	C(12)–C(13)–B(14)
B(4)–Li–O(26)	129.1(12)	B(5)–Li–O(26)	128.5(12)	C(12)–C(13)–B(17)	66.1(7)	B(14)–C(13)–B(17)
B(15)–Li–O(26)	131.5(13)	B(16)–Li–O(26)	132.2(13)	C(12)–C(13)–C(17)	119.4(9)	B(14)–C(13)–C(17)
C(3)–C(2)–B(6)	107.7(8)	C(3)–C(2)–B(7)	63.3(6)	B(17)–C(13)–C(17)	126.3(9)	C(13)–B(14)–B(15)
B(6)–C(2)–B(7)	63.3(6)	C(2)–C(3)–B(4)	115.0(8)	C(13)–B(14)–B(17)	59.0(7)	B(15)–B(14)–B(17)
C(2)–C(3)–B(7)	66.3(7)	B(4)–C(3)–B(7)	66.1(8)	B(14)–B(15)–B(16)	105.8(9)	B(14)–B(15)–B(17)
C(2)–C(3)–C(7)	119.7(9)	B(4)–C(3)–C(7)	123.1(9)	B(16)–B(15)–B(17)	61.2(7)	C(12)–B(16)–B(15)
B(7)–C(3)–C(7)	124.5(8)	C(3)–B(4)–B(5)	103.3(10)	C(12)–B(16)–B(17)	62.6(7)	B(15)–B(16)–B(17)
C(3)–B(4)–B(7)	62.6(8)	B(5)–B(4)–B(7)	60.7(8)	C(12)–B(17)–C(13)	51.5(6)	C(12)–B(17)–B(14)
B(4)–B(5)–B(6)	107.1(9)	B(4)–B(5)–B(7)	62.8(8)	C(13)–B(17)–B(14)	53.2(7)	C(12)–B(17)–B(15)
B(6)–B(5)–B(7)	63.9(8)	C(2)–B(6)–B(5)	106.8(8)	C(13)–B(17)–B(15)	92.8(8)	B(14)–B(17)–B(15)
C(2)–B(6)–B(7)	63.5(6)	B(5)–B(6)–B(7)	62.4(8)	C(12)–B(17)–B(16)	51.7(9)	C(13)–B(17)–B(16)
C(2)–B(7)–C(3)	50.4(5)	C(2)–B(7)–B(4)	91.2(7)	B(14)–B(17)–B(16)	95.3(8)	B(15)–B(17)–B(16)
C(3)–B(7)–B(4)	51.2(7)	C(2)–B(7)–B(5)	92.8(7)	Zr–O(21)–C(22)	124.4(5)	Zr–O(21)–C(25)
Compound IV						
Cnt(5)–Zr–Cl	107.9	Cnt(6)–Zr–Cl	109.4	B(14)–C(13)–B(17)	64.1(6)	C(13)–B(14)–B(15)
Cnt(5)–Zr–O(41)	104.6	Cnt(6)–Zr–O(41)	104.6	C(13)–B(14)–B(17)	62.9(5)	B(15)–B(14)–B(17)
Cnt(5)–Zr–Cnt(6)	130.5	Cl–Zr–O(41)	93.1(1)	B(14)–B(15)–B(16)	105.9(7)	B(14)–B(15)–B(17)
C(3)–C(2)–B(6)	111.9(7)	C(3)–C(2)–B(7)	64.6(5)	B(16)–B(15)–B(17)	63.0(6)	C(12)–B(16)–B(15)
B(6)–C(2)–B(7)	65.2(6)	C(2)–C(3)–B(4)	110.6(7)	C(12)–B(16)–B(17)	61.1(5)	B(15)–B(16)–B(17)
C(2)–C(3)–B(7)	63.8(5)	B(4)–C(3)–B(7)	65.5(6)	C(12)–B(17)–C(13)	52.2(4)	C(12)–B(17)–B(14)
C(3)–B(4)–B(5)	106.6(7)	C(3)–B(4)–B(7)	61.0(5)	C(13)–B(17)–B(14)	53.0(5)	C(12)–B(17)–B(15)
B(5)–B(4)–B(7)	62.2(6)	B(4)–B(5)–B(6)	104.7(7)	C(13)–B(17)–B(15)	94.9(6)	B(14)–B(17)–B(15)
B(4)–B(5)–B(7)	62.2(6)	B(6)–B(5)–B(7)	61.8(6)	C(12)–B(17)–B(16)	53.6(5)	C(13)–B(17)–B(16)
C(2)–B(6)–B(5)	106.2(7)	C(2)–B(6)–B(7)	60.9(5)	B(14)–B(17)–B(16)	96.0(6)	B(15)–B(17)–B(16)
B(5)–B(6)–B(7)	62.8(6)	C(2)–B(7)–C(3)	51.6(5)	Zr–O(41)–C(42)	125.5(5)	Zr–O(41)–C(45)
C(2)–B(7)–B(4)	92.4(6)	C(3)–B(7)–B(4)	53.5(5)	O(51)–Mg–O(56)	88.5(2)	O(51)–Mg–O(61)
C(2)–B(7)–B(5)	95.5(6)	C(3)–B(7)–B(5)	95.9(6)	O(56)–Mg–O(61)	89.4(2)	O(51)–Mg–O(51A)
B(4)–B(7)–B(5)	55.6(5)	C(2)–B(7)–B(6)	53.9(5)	O(56)–Mg–O(51A)	91.5(2)	O(61)–Mg–O(51A)
C(3)–B(7)–B(6)	93.4(6)	B(4)–B(7)–B(6)	95.4(6)	O(56)–Mg–O(56A)	180.0(1)	O(61)–Mg–O(56A)
B(5)–B(7)–B(6)	55.5(5)	C(13)–C(12)–B(16)	111.5(6)	Mg–O(51)–C(52)	123.8(5)	Mg–O(51)–C(55)
C(13)–C(12)–B(17)	64.4(5)	B(16)–C(12)–B(17)	65.3(6)	Mg–O(56)–C(57)	125.7(5)	Mg–O(56)–C(60)
C(12)–C(13)–B(14)	110.0(6)	C(12)–C(13)–B(17)	63.4(5)	Mg–O(61)–C(62)	127.4(4)	Mg–O(61)–C(65)
Compound V						
Cnt(7)–Zr–Cl(1)	108.1	Cnt(8)–Zr–Cl(1)	106.0	B(17)–C(13)–Si(4)	122.9(15)	C(13)–B(14)–B(15)
Cnt(7)–Zr–C(41)	102.7	Cnt(8)–Zr–C(41)	106.7	C(13)–B(14)–B(17)	63.5(15)	B(15)–B(14)–B(17)
Cnt(7)–Zr–Cnt(8)	132.0	Cl(1)–Zr–C(41)	95.3(4)	B(14)–B(15)–B(16)	106.6(16)	B(14)–B(15)–B(17)
B(4)–Li–B(14)	84.1(13)	B(5)–Li–B(14)	99.3(15)	B(16)–B(15)–B(17)	64.9(14)	C(12)–B(16)–B(15)
B(4)–Li–B(15)	98.9(14)	B(5)–Li–B(15)	86.6(13)	C(12)–B(16)–B(17)	60.4(13)	B(15)–B(16)–B(17)
B(5)–Li–Cl(4)	134.2(17)	B(14)–Li–Cl(4)	125.0(15)	C(12)–B(17)–C(13)	50.2(12)	C(12)–B(17)–B(14)
B(15)–Li–Cl(4)	134.0(16)	Zr–C(41)–Si(5)	132.2(7)	C(13)–B(17)–B(14)	51.6(13)	C(12)–B(17)–B(15)
C(3)–C(2)–B(6)	110.6(14)	C(3)–C(2)–B(7)	65.2(12)	C(13)–B(17)–B(15)	94.3(15)	B(14)–B(17)–B(15)
B(6)–C(2)–B(7)	64.3(12)	C(3)–C(2)–Si(1)	128.5(13)	C(12)–B(17)–B(16)	55.1(13)	C(13)–B(17)–B(16)
B(6)–C(2)–Si(1)	119.0(12)	B(7)–C(2)–Si(1)	125.7(12)	B(14)–B(17)–B(16)	94.3(16)	B(15)–B(17)–B(16)
C(2)–C(3)–B(4)	111.6(15)	C(2)–C(3)–B(7)	63.7(12)	Cl(2)–Mg(1)–Cl(3)	84.4(2)	Cl(2)–Mg(1)–Cl(4)
B(4)–C(3)–B(7)	64.7(13)	C(2)–C(3)–Si(2)	130.2(14)	Cl(3)–Mg(1)–Cl(4)	82.7(2)	Cl(2)–Mg(1)–O(51)
B(4)–C(3)–Si(2)	115.6(13)	B(7)–C(3)–Si(2)	125.6(13)	Cl(3)–Mg(1)–O(51)	95.6(5)	Cl(4)–Mg(1)–O(51)
C(3)–B(4)–B(5)	107.2(16)	C(3)–B(4)–B(7)	62.9(13)	Cl(2)–Mg(1)–O(56)	93.4(4)	Cl(3)–Mg(1)–O(56)
B(5)–B(4)–B(7)	62.8(13)	B(4)–B(5)–B(6)	105.2(15)	Cl(4)–Mg(1)–O(56)	89.9(4)	O(51)–Mg(1)–O(56)
B(4)–B(5)–B(7)	62.1(13)	B(6)–B(5)–B(7)	61.5(12)	Cl(2)–Mg(1)–O(61)	175.3(5)	Cl(3)–Mg(1)–O(61)
C(2)–B(6)–B(5)	105.4(14)	C(2)–B(6)–B(7)	61.4(12)	Cl(4)–Mg(1)–O(61)	95.3(5)	O(51)–Mg(1)–O(61)
B(5)–B(6)–B(7)	62.4(12)	C(2)–B(7)–C(3)	51.2(11)	O(56)–Mg(1)–O(61)	90.9(5)	Cl(2)–Mg(2)–Cl(3)
C(2)–B(7)–B(4)	92.5(14)	C(3)–B(7)–B(4)	52.4(12)	Cl(2)–Mg(2)–Cl(4)	83.3(2)	Cl(3)–Mg(2)–Cl(4)
C(2)–B(7)–B(5)	95.5(14)	C(3)–B(7)–B(5)	93.6(14)	Cl(2)–Mg(2)–O(66)	93.9(4)	Cl(3)–Mg(2)–O(66)
B(4)–B(7)–B(5)	55.0(12)	C(2)–B(7)–B(6)	54.2(11)	Cl(4)–Mg(2)–O(66)	175.8(4)	Cl(2)–Mg(2)–O(71)
C(3)–B(7)–B(6)	92.6(14)	B(4)–B(7)–B(6)	96.0(15)	Cl(3)–Mg(2)–O(71)	92.9(5)	Cl(4)–Mg(2)–O(71)
B(5)–B(7)–B(6)	56.1(12)	C(13)–C(12)–B(16)	110.6(17)	O(66)–Mg(2)–O(71)	92.5(5)	Cl(2)–Mg(2)–O(76)
C(13)–C(12)–B(17)	65.4(15)	B(16)–C(12)–B(17)	64.5(14)	Cl(3)–Mg(2)–O(76)	173.4(4)	Cl(4)–Mg(2)–O(76)
C(13)–C(12)–Si(3)	132.4(16)	B(16)–C(12)–Si(3)	115.8(15)	O(66)–Mg(2)–O(76)	91.6(5)	O(71)–Mg(2)–O(76)
B(17)–C(12)–Si(3)	127.1(14)	C(12)–C(13)–B(14)	111.5(17)	Mg(1)–Cl(2)–Mg(2)	80.7(2)	Mg(1)–Cl(3)–Mg(2)
C(12)–C(13)–B(17)	64.4(14)	B(14)–C(13)–B(17)	64.9(15)	Li–Cl(4)–Mg(1)	144.4(9)	Li–Cl(4)–Mg(2)
C(12)–C(13)–Si(4)	125.7(16)	B(14)–C(13)–Si(4)	119.5(15)	Mg(1)–Cl(4)–Mg(2)	78.1(2)	137.4(8)

^a Legend: Cnt(1) and Cnt(2) are the centroids of the C₂B₃ rings of I and Cnt(3) and Cnt(4) for II, Cnt(5) and Cnt(6) for IV, and Cnt(7) and Cnt(8) for V, respectively.

Scheme 1



Crystal Structures of I-THF, II, IV, and V. The solid-state structures of I-THF, II, IV, and V are shown in Figures 1–5, respectively. The unit cell of IV (Figure 4) shows that the two zirconacarborane anions are well separated and symmetrically placed on either side of a

solvated magnesium cation, giving a total population of four metallacarborane anions, two $[Mg(\text{THF})_6]^{2+}$ cations, and eight additional solvated THF's. In Figure 3, the $[Mg(\text{THF})_6]^{2+}$ cation is deleted, and only one of the two equivalent chlorozirconacarboranes of IV is shown. Table 2 gives the atomic coordinates of the complexes, while some selected bond distances and bond

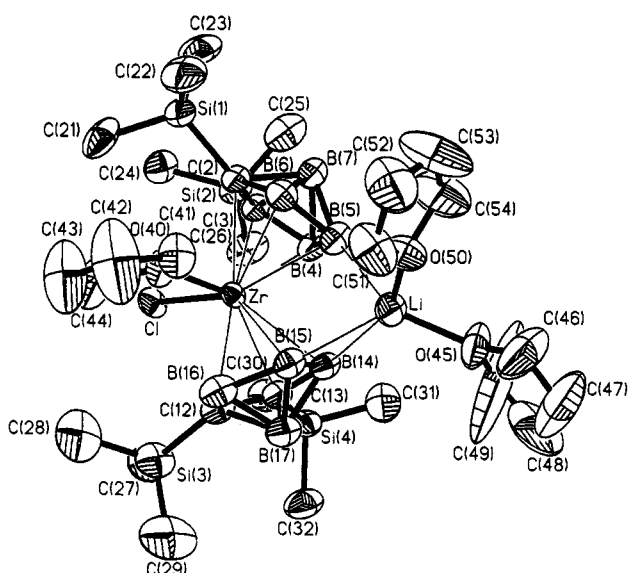


Figure 1. Perspective view of 1-Cl-1-(THF)-2,2',3,3'-($SiMe_3$)₄-4,5,5'-Li(THF)₂-1,1'-*commo*- $Zr(2,3-C_2B_4H_4)_2$ (**I-THF**) showing the atom-numbering scheme. The thermal ellipsoids are drawn at the 40% probability level. The $SiMe_3$, THF, and the cage H's are omitted for clarity.

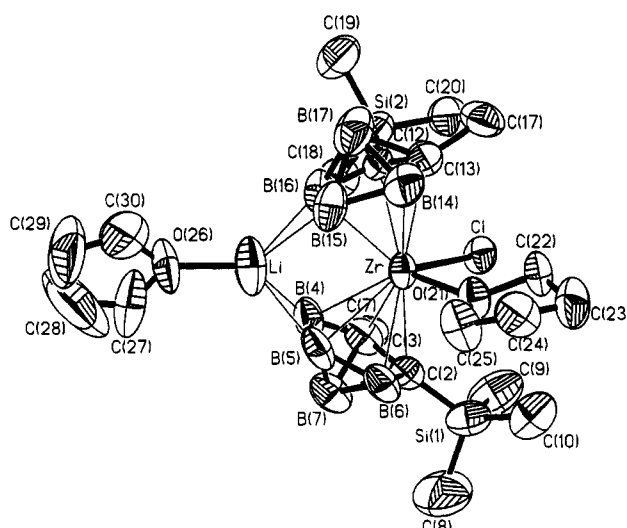


Figure 2. Perspective view of 1-Cl-1-(THF)-2,2'-($SiMe_3$)₂-3,3'-(Me)₂-4,4',5,5'-Li(THF)-1,1'-*commo*- $Zr(2,3-C_2B_4H_4)_2$ (**II**) showing the atom-numbering scheme. The thermal ellipsoids are drawn at the 40% probability level. The $SiMe_3$, THF, and cage H's are omitted for clarity.

Table 4. FT NMR Spectral Data^a

compd	δ splitting, assignt [$^1J(^{11}B-^1H)$ or $^1J(^{13}C-^1H)$, Hz]	rel area
I	200.13-MHz 1H NMR Data 3.82, s, THF; 3.6, br, ill-defined peak, basal H [$^1J(^{11}B-^1H)$ unresolved]; 3.35, s, THF; 2.6, br, ill-defined peak, apical H [$^1J(^{11}B-^1H)$ unresolved]; 1.15, s, THF; 1.09, s, THF; 0.30, s, Me ₃ Si; 0.21, s, Me ₃ Si	2:3:2:1:2:2:9:9
II	4.15, s, THF; 3.90, br, ill-defined peak, basal H [$^1J(^{11}B-^1H)$ unresolved]; 3.62, s, THF; 2.83, br, ill-defined peak, apical H [$^1J(^{11}B-^1H)$ unresolved]; 2.68, s, Me; 2.60, s, Me; 1.33, s, THF; 1.24, s, THF; 0.52, s, Me ₃ Si; 0.47, s, Me ₃ Si	4:6:4:2:3:3:4:4:9:9
III	6.44, s, cage CH; 4.04, br, ill defined peak, basal H [$^1J(^{11}B-^1H)$ unresolved]; 3.67, s, THF; 1.8, br, ill-defined peak, apical H [$^1J(^{11}B-^1H)$ unresolved]; 1.42, s, THF; 0.46, s, Me ₃ Si	1:3:4:1:4:9
IV ^b	3.57, br, THF; 1.60, br, THF; 0.42, s, Me ₃ Si	2:2:3
V ^b	3.73, s, THF; 3.60, br, ill-defined peak, basal H [$^1J(^{11}B-^1H)$ unresolved]; 1.78, s, THF; 1.6, br, ill-defined peak, apical H [$^1J(^{11}B-^1H)$ unresolved]; 0.61, s, Me ₃ Si-C _{cage} ; 0.57, s Me ₃ Si-C _{cage} ; 0.45, s, Me ₃ Si; 0.11, s, CH ₂ ,	12:3:12::1:9:9:4:5:1
	64.21-MHz ^{11}B NMR Data ^c	
I	33.16, br, ill-defined peak, basal BH [$^1J(B-H)$ unresolved]; 25.48, br, ill-defined peak, basal BH [$^1J(B-H)$ unresolved]; -16.32, br, ill-defined peak, apical BH [$^1J(B-H)$ unresolved]	1:2:1
II	30.08, br, basal BH [$^1J(B-H)$ unresolved]; 22.65, br, basal BH [$^1J(B-H)$ unresolved]; -14.04, d (br), apical BH (120)	1:2:1
III	28.80, vbr, ill-defined peak, basal BH [$^1J(B-H)$ unresolved]; 22.69, br, basal BH [$^1J(B-H)$ unresolved]; -17.27, br, apical BH [$^1J(B-H)$ unresolved]	1:2:1
IV	30.0, vbr, basal BH [$^1J(B-H)$ unresolved]; 24.0, br, basal BH [$^1J(B-H)$ unresolved]; -16.6, br, apical BH [$^1J(B-H)$ unresolved]	1:2:1
V	29.47, br, ill-defined peak, basal BH [$^1J(B-H)$ unresolved]; 19.86, br, ill-defined peak, basal BH [$^1J(B-H)$ unresolved]; -19.83, br, ill-defined peak, apical BH [$^1J(B-H)$ unresolved]	1:2:1
	50.32-MHz ^{13}C NMR data ^{a,d}	
I	123.92, s (br), cage C(SiCB); 123.42, s (br), cage C(SiCB); 76.43, t, Zr-THF(150); 68.63, t, Li-THF(148); 33.24, t, Zr-THF(127); 25.49, t, Li-THF(134); 3.65, q, Me ₃ Si (119.8); 3.25, q, Me ₃ Si (118.8)	1:1:1:1:1:1:3:3
II	123.03, s(br), cage C(SiCB); 119.91, s(br), cage C(MeCB); 119.03, s(br), cage C(MeCB); 76.06, t, Zr-THF(154.5); 69.03, t, Li-THF (149.3); 25.40, t, Zr-THF(135); 25.28, t, Li-THF(134); 24.29, q, Me (127); 22.93, q, Me (126.2); 2.15, q, Me ₃ Si (118)	2:1:1:2:2:2:2:1:1:6
III	117.96, s (br), cage C(SiCB); 113.85, d (br), cage C(HCB)(181.28); 76.46, t, Zr-THF(155.1); 69.07, t, Li-THF(147.5); 25.44, t, THF(133.3); 0.10, q, Me ₃ Si (119.51)	2:2:2:2:4:6
IV	116.36, s, cage C(SiCB); 66.57, m, THF; 24.35, m, THF; 3.19, q, Me ₃ Si (122.5)	1:3:3:3
V	116.78, s, cage C(SiCB); 113.2, s, cage C(SiCB); 112.5, s, cage C (SiBC); 68.12, m, THF; 25.68, m, THF; 4.43, q, C-SiMe ₃ (118.16); 4.30, q, C-SiMe ₃ (118.16); 3.91, q, C-SiMe ₃ (120.32); 1.99, q, Me ₃ Si (119.8); 0.16, t, CH ₂ (104.7)	2:1:1:12:12:3:3:6:3:1
	77.7-MHz 7Li NMR Data ^e	
I	-0.96	
II	-0.34	
V	-1.70	

^a C₆D₆ was used as solvent and as an internal standard with δ 7.15 ppm (in the 1H NMR spectra) and δ 128.0 ppm (in the ^{13}C NMR spectra) for compounds, with a positive sign indicating a downfield shift. ^b C₄D₈O was used as solvent. Legend: s = singlet, d = doublet, t = triplet, q = quartet, v = very, br = broad. ^c Shifts relative to external BF₃OEt₂. ^d Since relaxations of the cage carbons are slower than that of a protonated C, the relative areas of these carbons could not be measured accurately. ^e Shifts relative to external aqueous LiNO₃.

angles are listed in Table 3. An inspection of Table 3 shows that the structures of all the chlorozirconacarboranes are quite similar; therefore, unless otherwise noted, average bond distances and bond angles will be quoted. Each structure shows that the zirconium, in a formal +4 oxidation state, is sandwiched between two *nido*-C₂B₄ cages. The pentagonal C₂B₃ bonding faces are essentially planar, and the Zr is η^5 -bonded to the ring atoms; the average Zr-ring atom distance is $2.559 \pm 0.018 \text{ \AA}$.¹⁴ The Zr-Cent distance is $2.170 \pm 0.018 \text{ \AA}$ (Cent = the C₂B₃ ring centroid), which is greater than the Zr-Cent distances of 2.045 and 2.091 \AA found for the mixed-sandwich complexes (Cp*)(C₂B₉H₁₁)Zr[C-(Me)=CMe₂] and [(Cp*)(C₂B₉H₁₁)Zr]₂(μ -CH₂), respectively.⁴ The zirconacarboranes in this study are similar to the zirconocenes in that they are bent-sandwich complexes with Cent-Zr-Cent angles ranging from 130.4° for I-THF to 133.6° for II (see Table 3). Analogous angles for the early-transition-metal Cp sandwich complexes range generally around 120°.¹⁵⁻¹⁷ The reason for the larger bending angles found in I-THF, II, IV, and V is not apparent and may not be significant,

since a large variation exists in the bending angles of the zirconocenes. For example, a bending angle of 140.7° was found for the zwitterionic complex Cp*₂Zr⁺-(*m*-C₆H₄)B⁻(C₆H₄Et)₃.¹⁸ The bending allows for the additional coordination of the Zr so that the zirconacarboranes in I-THF, II, IV, and V and, presumably, in III, also contain Zr-Cl and Zr-THF (I-THF, II, and IV) or Zr-CH₂SiMe₃ (V) bonds. This results in a very distorted tetrahedral geometry about the zirconium atom; the Cl-Zr-R angles (R = THF, CH₂SiMe₃) range from 90.5° for I-THF to 95.3° for V, which are considerably smaller than the Cent-Zr-Cent angles (see Table 3). The average Zr-Cl bond distance in I-THF, II, IV, and V is $2.467 \pm 0.011 \text{ \AA}$, which is quite similar to the Zr-Cl distances of 2.452 \AA and 2.447 \AA for (η^5 -C₅H₄-XMe₃)Zr[CH(SiMe₃)₂]Cl, (X = C, Si, respectively) and the value of 2.441 \AA in [(η^5 -C₅H₄)₂(CH₂)₃]ZrCl₂.¹⁹ The

(16) (a) Bush, M. A.; Sim, G. A. *J. Chem. Soc. A* 1971, 2225. (b) Jeffery, J.; Lappert, M. F.; Luong-Thi, N. T.; Webb, M.; Atwood, J. L.; Hunter, W. E. *J. Chem. Soc. Dalton Trans.* 1981, 1593. (c) Lappert, M. F.; Riley, P. I.; Yarrow, P. I. W.; Atwood, J. L.; Hunter, W. E.; Zaworotko, M. J. *J. Chem. Soc., Dalton Trans.* 1981, 814.

(17) Crowther, D. J.; Borkowsky, S. L.; Swenson, D.; Meyer, T. Y.; Jordan, R. F. *Organometallics* 1993, 12, 2897.

(18) Hlatky, G. G.; Turner, H. W.; Eckman, R. R. *J. Am. Chem. Soc.* 1989, 111, 2728.

(19) Saldarriaga-Molina, C. H.; Clearfield, A.; Bernal, I. *J. Organomet. Chem.* 1974, 80, 79.

(14) The uncertainties given with the averages are the average deviations.

(15) Prout, K.; Cameron, T. S.; Forder, R. A.; Critchley, S. R.; Denton, B.; Rees, G. V. *Acta Crystallogr.* 1974, B30, 2290.

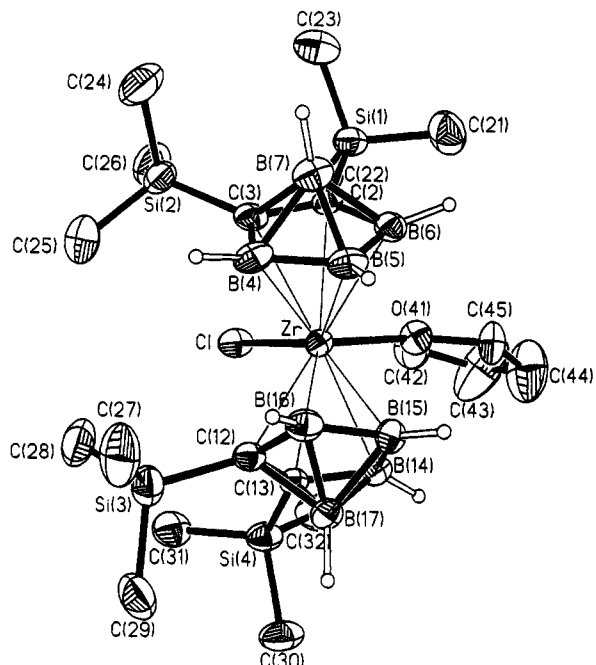


Figure 3. Perspective view of $[Mg(THF)_6][1\text{-Cl-}1\text{-(THF)}\text{-}2,2',3,3'\text{-(SiMe}_3)_4\text{1,1'-commo-Zr(2,3-C}_2\text{B}_4\text{H}_4)_2\text{]}_2\cdot 4\text{THF}$ (**IV**) showing the atom-numbering scheme. The thermal ellipsoids are drawn at the 40% probability level. The $[Mg(THF)_6]^{2+}$ cation and the THF's of crystallization are deleted, and only one of the two equivalent chlorozirconacarboranes of **IV** is shown. The SiMe_3 and THF H's are omitted for clarity.

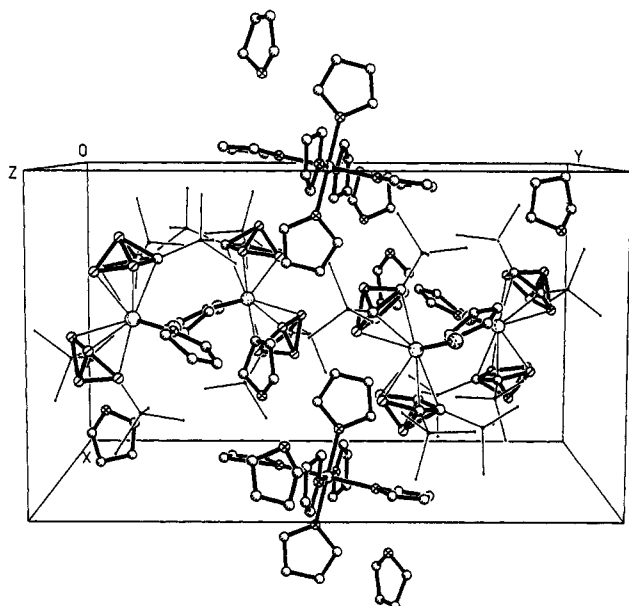


Figure 4. Crystal packing diagram of **IV**.

$Zr-\text{CH}_2\text{SiMe}_3$ distance of 2.271 Å in **V** is essentially the same as the values of 2.278 and 2.281 Å found for the analogous distances in $(\text{Cp})_2\text{Zr}(\text{CH}_2\text{SiMe}_3)_2$.^{16b} Coordination of the Cl^- ion in **I-THF-IV** imparts an overall negative charge to the zirconacarbonanes, while the additional coordination of the $[\text{CH}_2\text{SiMe}_3]^-$ in **V** results in a dianionic zirconacarbonane. In compounds **I-THF**, **II**, and **V**, charge compensation is accomplished by a Li^+ ion that bridges the two carborane cages of the zirconacarbonanes. The complexes differ in the connectivity of the Li to the cages and in the other groups bonded to the Li. Through a series of $\text{Li}-\text{H}-\text{B}$ bonds

in **II** and **V**, the Li is equally bridged between the basal and a unique boron on each carborane (the equivalent of B(4), B(5), B(15) and B(16) in Figure 2) and is also bonded to one other group, THF in **II** and $[\text{Mg}_2\text{Cl}_3\text{(THF)}_6]^{2+}$ in **V**. On the other hand, Figure 1 shows that the Li in **I-THF** is coordinated to two THF molecules and is equally bound to $\text{H-B}(14)$ and $\text{H-B}(15)$ (Li-B distances 2.45 ± 0.04 Å) and more weakly bound to $\text{H-B}(5)$ of the other cage (the $\text{Li-B}(5)$ distance is 2.61 Å). In all cases the Li groups bridge on the side of the carboranes located away from the large THF or CH_2SiMe_3 ligands. The bridged Li's do not seem to exert any systematic effect on the extent of bending of the complexes; Table 3 and Figures 3 and 4 show that the Cent-Zr-Cent bond angle of **IV**, which does not have bridging Li's, is essentially the same as that of **I-THF**, in which Li bridging exists.

Some insight into the substitutional inertness of **I** can be obtained by inspection of Figure 6, which shows the usual ball-and-stick model of **V** as well as a space-filling drawing of the complex at the same orientation. For clarity, the bridging Li group is not shown. It is apparent from Figure 6 that, even though the complex is bent, the SiMe_3 groups attached to the cage carbons of the carboranes effectively shield the Cl ligand so that any substitution process which has a large, or moderate, associative component to it would be greatly inhibited. The orientation of the cage carbons, and their attached derivative groups, above and below the Zr-bound Cl ligand is dictated by steric requirements. In these positions, the SiMe_3 groups are on the open side of the bent structure and away from the bulky THF (or CH_2SiMe_3) group; any change in the relative orientations of the carborane ligands should result in increased ligand-ligand repulsion.

Spectroscopy. All compounds were characterized by ^1H , ^{11}B , and ^{13}C pulse Fourier transform NMR spectra and IR spectra. Compounds **I**, **II**, and **V** were also characterized by ^7Li NMR spectroscopy. The results of these spectroscopic studies are given in Tables 4 and 5.

The ^1H NMR spectra of **I-V** show appropriate resonances for the carborane protons, those associated with SiMe_3 , Me, or H cage carbon substituents, and THF. In addition, **V** showed two sharp singlets at 0.45 and 0.11 ppm ascribed to the SiMe_3 and CH_2 protons of the $\text{Zr}-\text{CH}_2\text{SiMe}_3$ moiety, respectively (see Table 4). The 0.11 ppm peak is in the range reported for a number of Zr-bound methyl and methylene hydrogen resonances.^{20,21}

The ^{11}B NMR spectra of compounds **I-V** are all similar to one another and exhibit the characteristic three-peak pattern (1:2:1 peak area ratio) of the 1,2,3- MC_2B_4 cage metallacarboranes.³ Table 4 shows that all compounds have an apical boron (the equivalent of B(7) in Figure 1) resonance in the -14 to -20 ppm region and a unique boron (the equivalent of B(5) in Figure 1) resonance in the 20 to 25 ppm region, with the basal borons (the equivalent of B(4) and B(6) in Figure 1) having resonances around 29–33 ppm. Complexation of the *nido*-carborane dianionic ligands by zirconium draws electron density away from the cage, thereby deshielding the cage borons, which results in downfield

(20) Bochmann, M.; Lancaster, S. J.; Hursthouse, M. B.; Abdul Malik, K. M. *Organometallics* 1994, 13, 2235.

(21) Siedle, A. R.; Newmark, R. A.; Lamanna, W. M.; Schroepfer, J. N. *Polyhedron* 1990, 9, 301.

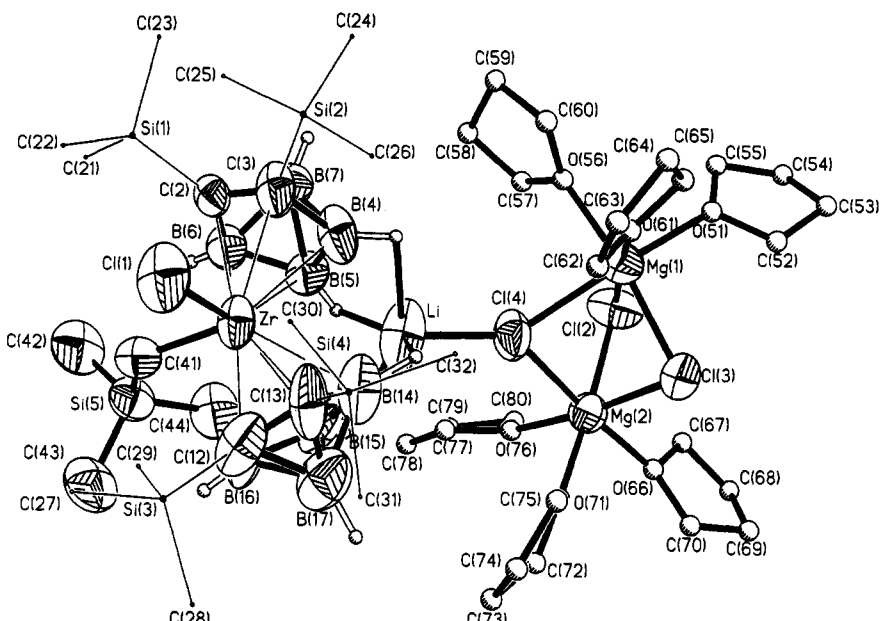


Figure 5. Perspective view of 1-Cl-1-(CH₂SiMe₃)-2,2',3,3'-(SiMe₃)₄-4,4',5,5'-(μ -H)₄Li](μ ₃-Cl)[Mg(μ ₂-Cl)(THF)₃]₂-1,1'-commo-Zr(2,3-C₂B₄H₄)₂ (**V**) showing the atom-numbering scheme. The thermal ellipsoids are drawn at the 40% probability level. The atoms of the C_{cage}-SiMe₃ and the THF groups are drawn with the circles of arbitrary radii. Except for the cage BH's, the H atoms are omitted for clarity.

Table 5. Infrared Absorptions (cm⁻¹)^a

I	2954 (vs), 2896 (sh) [ν (C—H)], 2543 (vs), 2496 (sh), 2449 (sh) [ν (B—H)], 1443 (w, br), 1402 (w, br) [δ (CH) _{asym}], 1355 (w, br), 1337 (w), 1249 (vs) [δ (CH) _{sym}], 1179 (ms), 1126 (w, br), 1067 (w, sh), 1044 (m), 1002 (m, br), 914 (w, sh), 844 (vvs, br) [ϱ (CH)], 761 (s, s), 703 (w, br), 632 (m, s), 602 (w, sh), 532 (w, br), 479 (w, br)
II	2941 (vs), 2880 (vs) [ν (C—H)], 2530 (vs), 2480 (vs), 2420 (vs, sh) [ν (B—H)], 2370 (w), 2260 (vs), 1610 (s), 1540 (vw), 1445 (s) [δ (CH) _{asym}], 1385 (w, br), 1360 (vw), 1325 (s), 1240 (vs), 1210 (m) [δ (CH) _{sym}], 1155 (w), 1060 (w, sh), 1030 (m), 995 (m), 935 (vw), 910 (w, sh), 845 (vvs, br) [ϱ (C—H)], 750 (s), 679 (m), 621 (m), 560 (w), 490 (vvs, br), 415 (w)
III	2940 (vs), 2880 (vs, sh) [ν (C—H)], 2520 (vs), 2440 (s, sh), 2340 (m, sh) [ν (B—H)], 2100 (w, br), 1465 (w), 1400 (w) [δ (CH) _{asym}], 1350 (w, br), 1240 (vs) [δ (CH) _{sym}], 1175 (m), 1130 (w, sh), 1075 (s, sh), 1035 (s), 990 (m, sh), 880 (vs), 840 (s, sh) [ϱ (CCH)], 770 (m, sh), 750 (s), 670 (m), 615 (m), 390 (m), 350 (w)
IV	2580 (m, sh), 2510 (vs) [ν (B—H)], 1400 (w, br), 1340 (w), 1310 (w), 1233 (s), 1160 (vw, sh), 1115 (vw), 1010 (w), 978 (w), 824 (vs), 752 (s), 678 (m), 625 (m), 600 (w), 520 (w) 428 (m), 405 (m)
V	3037–2813 (vs, br) [ν (C—H)], 2705 (s) [ν (C—H)], 2522 (m) [ν (B—H)], 2298 (w), 1973 (w), 1478 (vs) [δ (C—H)], 1369 (vs) [δ (C—H)], 1335 (s) [δ (C—H)], 1288 (vs), 1240 (vs), 1200 (vs), 1071 (vs, br), 894 (vs, br), 758 (s), 665 (s), 640 (s, sh), 507 (vs)

^a For **I–IV** C₆D₆ was used as solvent; THF was used for **V**; reference standard. Legend: v = very, s = strong or sharp, m = medium, w = weak, sh = shoulder, br = broad.

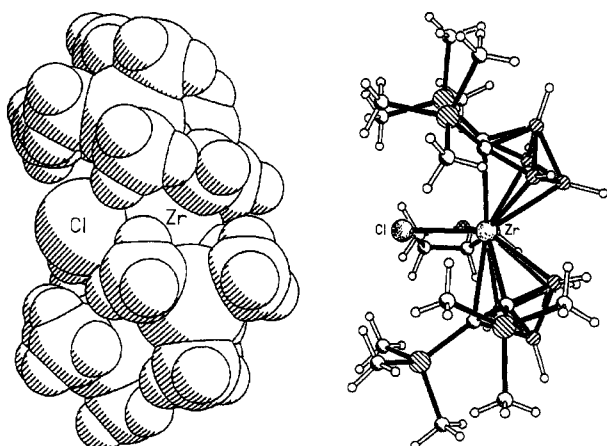


Figure 6. Space-filling and ball-and-stick models of **V** drawn at the same orientation showing a blockage of the Cl ligand by bulky SiMe₃ substituents on the cage carbons. The bridging groups are not shown for clarity.

shifts of the boron resonances by 20–30 ppm, from their positions in the ¹¹B NMR spectra of the starting Na/Li carboranes.^{10,11} These ¹¹B NMR shifts are similar to those found when other metals bond to the C₂B₄ carboranes and have been explained in terms of a

transfer of electron density out of the cages on metal coordination.²² In general, the peaks are much broader than those found in the Na/Li carborane precursors, hence accurate determinations of B—H coupling constants for compounds **I–V** could not be obtained.

The ¹³C NMR spectra of **I–III** show resonances for both Li-coordinated and Zr-coordinated THF molecules. For example, compound **I** has resonances at 76.43 and 33.24 ppm due to the carbons of the Zr—THF molecule, while the analogous resonances for the Li—THF molecule are at 68.63 and 25.49 ppm, respectively (see Table 4). These results are consistent with the solid-state structures of compounds **I** and **II**, which show that both the Zr and Li metals have coordinated THF molecules. Compound **IV**, which also has THF molecules attached to different metal centers (six bonded to a Mg and one bonded to Zr), exhibits only a single set of ¹³C resonances at 66.57 and 24.35 ppm. In all probability the Zr—THF resonances of this compound are masked by the more intense resonances due to the Mg-bound molecules. The ¹H NMR spectra of **I** and **II** parallel their ¹³C NMR results in that two sets of methylene hydrogens are found. For example, the ¹H NMR spectrum of **I** exhibits

(22) Hosmane, N. S.; Lu, K.-J.; Zhang, H.; Maguire, J. A.; Jia, L.; Barreto, R. D. *Organometallics* 1992, 11, 2458 and references therein.

one set at 3.82 and 1.15 ppm, associated with the Li-THF molecules and another at 3.6 and 1.09 ppm, attributable to the Zr-bound molecules. When the ^1H NMR spectrum of **I** was run as a function of time in a $\text{C}_4\text{D}_8\text{O}/\text{C}_6\text{D}_6$ mixture, the 3.82/1.15 ppm signals slowly disappeared, while the upfield set did not change, even after 5 days had elapsed. These observations indicate that exchange of the Li-bound THF molecules, while slow, is much faster than that of the Zr-bound molecules.

With the exception of compound **IV**, the ^{13}C NMR spectra of all the zirconacarborane cage carbons, and those of their substituent groups, showed multiple resonances indicating nonequivalent cage carbons (see Table 4). Since the cage carbons of **II** and **III** have different substituent groups attached (SiMe_3 , Me, or H), nonequivalence is expected. However, the splitting pattern in **II**, that is, three cage carbon resonances in a 2:1:1 peak area ratio, is more complex than would arise from just the different groups bonded to these atoms, and **I**, which has the same cage carbon substituents, also shows nonequivalent cage carbons. An inspection of various cage carbon-THF, -Cl, and -Li distances in the structures shown in Figures 1, 2, and 5 reveals that the cage carbons of a particular carborane are not equidistant from either the Zr-bound THF (or $\text{CH}_2\text{-SiMe}_3$) ligand or the bridging Li group. At this point it is not possible to assess the relative importance of the two inequalities in determining the multiplicity of the ^{13}C NMR resonances found in the zirconacarboranes. The fact that the ^{13}C NMR spectrum of compound **IV**, which does not have lithium bridges, shows equivalent cage carbons argues for the importance of lithium placement. However, it should be noted that, with the exception of compound **IV**, none of the solid-state structures correctly predicts the solution ^{13}C NMR spectra of the compounds investigated in this study. In addition, the observation that the resonances in both the ^{11}B and ^{13}C NMR spectra of **IV** are much sharper than those of the other zirconacarboranes suggests that some fluxionality involving the bridged lithium groups exists in solution. The ^7Li NMR spectra of **I**, **II**, and **V**

show single resonances at -0.96 , -0.34 , and -1.70 ppm, respectively, which are typical of *exo*-polyhedrally bound lithiums found in the group 1 C_2B_4 cage carboranes.^{11a,23}

The infrared spectra of the compounds show absorptions expected from the structures and formulas of the compounds. These absorptions are listed in Table 5 for the purposes of qualitative analysis.

Conclusion. Although the full-sandwich carboranes $1\text{-Cl-}1\text{-(THF)-}2,2'\text{-(SiMe}_3)_2\text{-}3,3'\text{-(R)}_2\text{-}4,4',5,5'\text{-Li(THF)-}1,1'\text{-commo-Zr(2,3-C}_2\text{B}_4\text{H}_4)_2$ ($\text{R} = \text{SiMe}_3$ (**I**), Me (**II**), H (**III**)) form readily and are structurally similar to the bent-sandwich chlorozirconocenes, they differ markedly in their reactivities. The coordinated chloride ligands in **I–III** were found to be substitutionally inert in the presence of the Grignard reagent $\text{Me}_3\text{SiCH}_2\text{MgCl}$ or other alkylating agents, such as AlMe_3 and LiR ($\text{R} = \text{Me}$, *t*-Bu, Me_3SiCH_2). The solid-state structures of **I**, **II**, and several of the reaction products of **I** and the Grignard reagent showed that the Cl ligand was well protected by the large SiMe_3 groups on the carborane cage carbons. The effects of different substituents on the cage carbons of the carborane ligands of the chlorozirconacarborane and chlorohafnacarborane sandwich complexes are currently under investigation in our laboratories.

Acknowledgment. This work was supported in part by grants from the Texas Advanced Technology Program (Grant No. 003613006), the National Science Foundation (Grant No. CHE-9400672), the Robert A. Welch Foundation (Grant No. N-1016), the Southern Methodist University Research Council, and the donors of the Petroleum Research Fund, administered by the American Chemical Society.

Supplementary Material Available: Tables of anisotropic thermal parameters and H atom positional parameters for **I**-THF, **II**, **IV**, and **V** (9 pages). Ordering information is given on any current masthead page.

OM9407767

(23) Wang, Y.; Zhang, H.; Maguire, J. A.; Hosmane, N. S. *Organometallics* **1993**, *12*, 3781.